EUROPEAN COOPERATION
IN SCIENCE AND TECHNOLOGY

Whitepaper on experimental and computational techniques

Minimum level of detail needed for reproducible science

Version 1.1, Sep. 7, 2016

COST Action CM1305 (ECOSTBio)

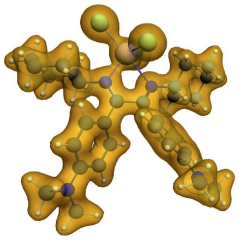

COST Action CM1305

ECOST3IO

Explicit Control Over Spin-states
in Technology and Biochemistry

Table of Contents

- 1. Interested parties
  - Coupled cluster/MBPT
  - DFT
  - Density Matrix Renormalization Group
  - Electrochemistry/Cyclic Voltammetry
  - Electrochemistry/Differential pulse voltammetry
  - Electrochemistry/Exhaustive electrolysis
  - Electron paramagnetic resonance
  - EXAFS
  - Infrared spectroscopy
  - Ligand-field Density Functional Theory
  - Magnetic circular dichroism
  - Mass spectrometry
  - Molecular dynamics
  - Molecular mechanics
  - Mössbauer
  - Multi-configurational wavefunctions
  - Multi-reference CI/Difference-dedicated CI
  - NMR
  - Photophysical and photochemical methods
  - QM/MM, Multi-level schemes
  - Raman and Resonance Raman spectroscopy
  - SQUID
  - Stopped-flow
  - Time-dependent DFT
  - UV-Vis
  - Vibrational circular dichroism
  - X-ray absorption
  - X-ray emission
- 2. Description of techniques and current issues
  - Coupled cluster/MBPT
  - DFT
  - Density Matrix Renormalization Group
  - Electrochemistry/Cyclic Voltammetry
  - Electrochemistry/Differential pulse voltammetry
  - Electrochemistry/Exhaustive electrolysis
  - Electron paramagnetic resonance
  - Infrared spectroscopy
  - Ligand-field Density Functional Theory
  - Magnetic circular dichroism
  - Mass spectrometry
  - Molecular dynamics
  - Molecular mechanics
  - Mössbauer
  - Multi-configurational wavefunctions
  - Multi-reference CI/Difference-dedicated CI
  - NMR
  - Photophysical and photochemical methods
  - QM/MM, Multi-level schemes

Raman and Resonance Raman spectroscopy
SQUID
Stopped-flow
Time-dependent DFT
UV-Vis
Vibrational circular dichroism
X-ray absorption
X-ray emission
3. Descriptors with information
General
Coupled cluster/MBPT
DFT
Density Matrix Renormalization Group
Electrochemistry/Cyclic Voltammetry
Electrochemistry/Differential pulse voltammetry
Electrochemistry/Exhaustive electrolysis
Electron paramagnetic resonance
Infrared spectroscopy
Ligand-field Density Functional Theory
Magnetic circular dichroism
Mass spectrometry
Molecular dynamics
Molecular mechanics
Mössbauer
Multi-configurational wavefunctions
Multi-reference CI/Difference dedicated CI
NMR
Photophysical and photochemical methods
QM/MM, Multi-level schemes
Raman and Resonance Raman spectroscopy
SQUID
Stopped-flow
Time-dependent DFT
UV-Vis
Vibrational circular dichroism
X-ray absorption
X-ray emission

1. Interested parties

Coupled cluster/MBPT

Stephan Sauer (rapporteur)
Mariusz Radoń (main author)
Tibor Szilvási
Jeremy Harvey
Kasper Kepp
Kenneth Ruud
Julianna Olah
Mariona Sodupe
Leeor Kronik
Dimitrios Pantazis
Quan Phung
Kristine Pierloot
Markus Reiher

DFT

Marcel Swart (rapporteur)
Sam de Visser
Kasper Kepp
Rob Deeth
Leeor Kronik
Peter Comba
Paola Belanzoni
Stephan Sauer
David Balcells
Tomasz Borowski
Leticia Gonzalez
Jeremy Harvey
Ulf Ryde
Coen de Graaf
Ewa Broclawik
Carmen Sousa
Mariusz Radoń
Balazs Pinter
Pablo Garcia-Fernandez
Wybren Jan Buma
Dimitrios Pantazis
Edwin Otten
Giovanni La Penna
Amelie Kochem
Tibor Szilvási
Davide Angelone
Mariona Sodupe
Maylis Orio
Bas de Bruin
Pascale Maldivi
Quan Phung
Kristine Pierloot
Maja Gruden
Matija Zlatar

Markus Reiher

Density Matrix Renormalization Group

Markus Reiher (rapporteur)
Lubomír Rulíšek
Tibor Szilvási
Leticia Gonzalez
Kristine Pierloot
Quan Phung

Electrochemistry/Cyclic Voltammetry

Wesley Browne (rapporteur)
Karsten Meyer
Panayotis Kyritsis
Patrina Paraskevopoulou
Marcello Gennari
Christelle HUREAU
Emira Kahrović
Edwin Otten
Chloe Johnson
Dominique Mandon

Electrochemistry/Differential pulse voltammetry

Wesley Browne (rapporteur)

Electrochemistry/Exhaustive electrolysis

Wesley Browne (rapporteur)

Electron paramagnetic resonance

Carole Duboc (rapporteur)
Malcolm Halcrow
Peter Comba
Jalila Simaan
Grace Morgan
Karsten Meyer
Hans-Jörg Krüger
Marcello Gennari
Frederic Banse
Christelle HUREAU
Dijana Zilic
Jean-Marc Latour
Dominique Mandon
Amelie Kochem
Maylis Orio
Bas de Bruin
Panayotis Kyritsis
Aidan McDonald
Edwin Otten
Ana Popovic
Stephan Sauer
Dijana Zilic

Infrared spectroscopy

Grace Morgan (rapporteur)
Panayotis Kyritsis
Ewa Broclawik
Patrina Paraskevopoulou
Hans-Jörg Krüger
Emira Kahrović
Davide Angelone
Peter Weinberger
Bas de Bruin
Aidan McDonald
Iztok Turel

Ligand-field Density Functional Theory

Maja Gruden (rapporteur)
Rob Deeth
Claude Daul
Peter Comba
Matija Zlatar

Magnetic circular dichroism

Wybren Jan Buma (rapporteur)

Mass spectrometry

Jana Roithova
Iztok Turel

Molecular dynamics

Michele Cascella (rapporteur)
Ferran Feixas
Kasper Kepp
Tomasz Borowski
Leticia Gonzalez
Julianna Olah
Carme Rovira
Coen de Graaf
Alex Domingo
Giovanni La Penna
Mariona Sodupe

Molecular mechanics

Rob Deeth (rapporteur)
Peter Comba
Marcel Swart
Maja Gruden

Mössbauer

Peter Weinberger (rapporteur)
Franc Meyer
Karsten Meyer
Paulo Martinho

Jean-Marc Latour
Birgit Weber
Hans-Jörg Krüger
Peter Weinberger
Yann Garcia
Stephan Sauer
Markus Reiher

Multi-configurational wavefunctions

Kristine Pierloot (rapporteur)
Coen de Graaf
Kasper Kepp
Peter Comba
Leticia Gonzalez
Markus Reiher
Ewa Broclawik
Carmen Sousa
Mariusz Radoń
Alex Domingo
Tibor Szilvási
Mariona Sodupe
Maylis Orio
Quan Phung
Lubomír Rulíšek

Multi-reference CI/Difference-dedicated CI

Kenneth Ruud (rapporteur)
Stephan Sauer
Markus Reiher
Coen de Graaf
Pablo Garcia-Fernandez
Leticia Gonzalez
Dimitrios Pantazis
Alex Domingo
Tibor Szilvási
Maylis Orio

NMR

Ricardo Louro (rapporteur)
Malcolm Halcrow
Peter Comba
Franc Meyer
Aidan McDonald
Grace Morgan
George Britovsek
Paulo Martinho
Panayotis Kyritsis
Patrina Paraskevopoulou
Iztok Turel
Marcello Gennari
Vladimir Arion
Christelle HUREAU
Paolo Pirovano
Edwin Otten

Chloe Johnson
Dominique Mandon
Amelie Kochem
Bas de Bruin
Stephan Sauer

Photophysical and photochemical methods

Marcello Gennari (rapporteur)
Wesley Browne

QM/MM, Multi-level schemes

Matthias Stein (rapporteur)
Sam de Visser
Marcel Swart
Kenneth Ruud
Michele Cascella
David Balcells
Tomasz Borowski
Julianna Olah
Ulf Ryde
Carme Rovira
Kasper Kepp
Maja Gruden

Raman and Resonance Raman spectroscopy

Wesley Browne (rapporteur)
Yann Garcia
Grace Morgan
Hans-Jörg Krüger
Davide Angelone
John McGarvey
Aidan McDonald
Markus Reiher

SQUID

Grace Morgan (rapporteur)
Yann Garcia
Malcolm Halcrow
Peter Comba
Franc Meyer
Birgit Weber
Karsten Meyer
Paulo Martinho
Dominique LUNEAU
Marie Sircoglou
Peter Weinberger

Stopped-flow

Jalila Simaan (rapporteur)
Marie Sircoglou
Frederic Banse
Jean-Marc Latour

Time-dependent DFT

Benoit Champagne (rapporteur)
Michele Cascella
Kenneth Ruud
Matthias Stein
Markus Reiher
Dimitrios Pantazis
Maja Gruden
Matija Zlatar

UV-Vis

Kallol Ray (rapporteur)
Peter Comba
Christian Enachescu
Aidan McDonald
Grace Morgan
George Britovsek
Panayotis Kyritsis
Patrina Paraskevopoulou
Hans-Jörg Krüger
Frederic Banse
Emira Kahrović
Paolo Pirovano
Chloe Johnson
Dominique Mandon
Amelie Kochem
Davide Angelone
Peter Weinberger
Bas de Bruin
Iztok Turel

Vibrational circular dichroism

Wybren Jan Buma (rapporteur)

X-ray absorption

Serena DeBeer (rapporteur)
Kallol Ray
Ulf Ryde

X-ray emission

Serena DeBeer (rapporteur)

2. Description of techniques and current issues

Coupled cluster/MBPT

Coupled cluster (CC) and many-body perturbation theory (MBPT) methods are among the most accurate and reliable computational approaches in molecular electronic structure theory[1]. These methods provide an approximate solution to the Schrödinger equation for the ground state (more generally: for the lowest state with a given spin multiplicity and spatial symmetry); the treatment of excited states (with the same multiplicity and symmetry as the ground state) is made possible by using EOM-CC (equation-of-motion)[2] or CC linear response[3] approaches. Due to their high computational cost CC methods are not yet routinely applicable for larger systems. Furthemore the standard CC methods are essentially single-reference methods, which also restricts their application.

Within CC theory the effects of electronic correlation are treated very efficiently by the choice of the so called exponential ansatz. The accuracy can be systematically improved by including in the cluster operator excitations up to increasingly higher orders, such as in the following sequence of methods: CCSD, CCSDT, CCSDTQ,…., which starts from the CC theory with connected singles and doubles amplitudes (CCSD), after which the triples (T), quadruples (Q), and also higher excitations can be gradually included. This sequence will ultimately converge to full CI (i.e., it will provide the exact solution of the Schrödinger equation within a given basis set). However, the computational cost increases rapidly with the order of excitations included, being the first very serious limitation for the wide of application of CC methods to chemical problems. Except for very small systems, it is impossible to include the quadruples (and higher excitations) and it is usually impractical to treat the triples iteratively. The triples are typically treated approximately (perturbatively) on top of the CCSD method, leading to the famous and the most popular CCSD(T) approach, which is often regarded as the "golden standard" of accuracy for a variety of chemical problems[4]. Examples of other CC methods that include the triples approximately are: completely-renormalized CR-CC(2,3) theory and CC3. As a rule of thumb, the inclusion of triples is mandatory for obtaining meaningful results, especially for transition metal compounds.

The CC and MBPT methods are implemented in many quantum chemical programs, like Gaussian, GAMESS, Molpro, Molcas, Turbomole, Orca, Psi4, CFour, Aces, Dalton, Dirac, NWChem and MRCC, to name some. However, the users should be aware that - especially for open-shell systems - the same acronym, like "CCSD(T)", may actually refer to slightly different theories in different programs. This is because the open-shell calculations can be based either on an UHF or ROHF wave function; and for the second choice the spin-unrestricted (UCCSD(T)) or partially spin-restricted (RCCSD(T)) formulation can be chosen. When reporting the results, the user is recommended to describe precisely which of these CC methods was used. Another possibility is to perform CC calculations based on DFT orbitals or other non-canonical orbitals, or to use Brückner orbitals; such a choice must always be explicitly mentioned when reporting the results.

All the CC and MBPT methods are computationally much more expensive than the widely used DFT methods (in terms of CPU time and resources: memory and disk). Full geometry optimizations at the CC level are rarely performed (except for small systems). The typical use these methods in (bio)inorganic chemistry is to perform single-point energy calculations for the structures earlier optimized at a computationally cheaper level (such as DFT). Even then, CC methods cannot be easily applied to larger systems and they are ineligible for routine application in the studies of reaction mechanisms – although such studies can certainly be performed at the CC level for smaller molecules and simplified model systems[5, 6], providing a valuable insight into reaction mechanisms beyond the DFT level.

The high computational cost is due to unfavorable scaling of CC/MBPT methods with the system size (e.g., N^7 for CCSD(T)) and can be significantly reduced by the local treatment of electron correlation[7-9]. Unfortunately, local CC codes which are publically available at the moment have typically certain limitations, e.g., they are restricted to closed-shell systems (preventing the treatment of spin states other than singlet) or the methods are not implemented beyond the CCSD level. It is expected that these

limitations will disappear in the near future, making the CC/MBPT machinery more routinely applicable to larger systems.

Another issue of the CC and MBPT methods is slow basis set convergence of the results. In conventional calculations very large basis set (quadruple-ζ and larger) is usually required to obtain meaningful results and extrapolation to complete basis set (CBS) may be necessary to reach the chemical accuracy (1-3 kcal/mol). Clearly, the use of large basis set makes the calculations much more expensive, sometimes impossible to perform. This bottleneck is remedied, in part, by using explicitly-correlated CC/MBPT methods[10, 11] (e.g., CCSD-F12, MP2-F12). These methods make it possible to obtain the results close to the CBS limit with a relatively small basis set[12]. When speaking about chemically-relevant relative energies, the triple-ζ basis set is usually enough and sometimes it may be even truncated to double-ζ basis set for regions of molecule not being directly involved in a given process or reaction[5, 13]. Owing to their clear advantages, the explicitly correlated CC methods are becoming increasingly popular. However, when using these methods the users have to pay their attention to a few additional details compared with conventional CC calculations (such as: selection of the auxiliary basis sets; the ansatz chosen for description of explicit correlation; CABS correction; which particular version of CCSD-F12 is used; how the triples contribution to the correlation energy is handled). Such details should always accompany the results to make them reproducible.

The standard CC and MBPT methods are single-reference, meaning that they employ only one Slater determinant as the starting point for constructing the correlated wave function. (There are also some multi-reference generalizations of CC methods and EOM-CC approaches applicable to multi-reference systems, but these methods are not covered in this short text.) Hence, single-reference CC/MBPT methods work best for systems for which a single determinant is a reasonable zero-order approximation to the wave function. However, there are also “multi-reference” problems where this condition is not met, either in principle (e.g., for weak antiferromagnetic coupling of electrons) or in a certain region of the potential energy surface (e.g., for dissociation of a covalent bond). For such systems the use of low order CC (and even more MBPT methods) should be avoided[14]. For instance, description of a bond dissociation curve is a typical case where CCSD, CCSD(T), and even CCSDT (especially for multiple bonds) may produce unreliable results. On the other hand, the popular CCSD(T) method is known to work well for many systems with a noticeable (albeit not extreme) multi-reference character, including some transition metal species near their equilibrium geometries[4].

Several metrics were introduced to quantify the amount of multi-reference character for a given system, including: T_1 and D_1 diagnostics based on the amplitudes of the singles; the analogous diagnostics based on the amplitudes of the doubles; the amount of spin-contamination in an unrestricted wave function; and the percentage contribution of the triples to the atomization energy[15]. If large values of these diagnostics are observed, the user should treat the CCSD(T) results with care and preferably compare them with the results of other (multi-reference, higher order CC) calculations. However, none of these diagnostics work perfectly and it is still not clear how their values could be translated into the “error bars” of computational results. For instance, there are systems where – despite relatively high values of the diagnostics – CCSD(T) results are still very reliable (compared with higher-order CC methods, multi-reference methods, or experimental data)[4]. Thus, in practice, the demarcation line between “single-reference” and “multi-reference” systems is not set as clearly as it might seem and many interesting systems fall in between the two classes. Hence, it is presently a major challenge to determine the accuracy of single-reference CC methods when applied to this “intermediate region”, where a number of transition metal complexes seem to fall in.

DFT

The rapporteur (M. Swart) says he will finish this soon.

One short paragraph as general description (including references to “Further reading”), plus a 1-3 page description of what are the current issues with the technique, which are limiting factors, and which kind of (technical) information is critical, what data is often overlooked, etc. etc.
PLEASE:

• include references between hashes, highlight them and preferably only DOIs, e.g. #DOI: 10.1021/ct800277a# or #C. Daul, M. Zlatar, M. Gruden-Pavlovic and M. Swart, "Application of Density Functional and Density Functional Based Ligand Field Theory to Spin States", In: Spin states in biochemistry and inorganic chemistry: Influence on Structure and Reactivity, M. Swart, M. Costas (Eds.), Wiley, 2015; Ch. 2, in press#.

Density Matrix Renormalization Group

The density matrix renormalization group (DMRG) is a method to optimize a matrix-product-state representation of the electronic wave function. Whereas it was originally developed for spin physics by White[16], the first applications to quantum chemistry were published in the late 1990s. It approximates the exact solution (FCI) in a given orbital space (CAS-CI). The DMRG wave function can be improved by also optimizing the orbital basis. As such, DMRG is a CASSCF-type method. Due to its polynomial scaling with system size, it does not hit the exponentially scaling wall of traditional CASSCF. This gives access to active spaces beyond the 18 electrons in 18 spatial orbitals limit of traditional CASSCF. In fact, DMRG scales with the number of orbitals so that complete active spaces (CAS; with ordered orbitals it is called 'lattice' in DMRG) of up to about 100 orbitals are accessible. This is achieved by a systematic dimension reduction characterized by the number of renormalized block states (often abbreviated as m or M, where 'block' refers to states defined on a subset of the CAS). Systematically, many-particle states are constructed on this subset (the 'system') and, in each step, the subset is enlarged by one orbital until all orbitals of the CAS are incorporated in the subset. This process is called a 'sweep' and once it is completed, its direction is reversed. Sweeping is continued until the total electronic energy is converged. As DMRG works iteratively, its convergence depends on some parameters. Hence, to specify the results of a DMRG calculation, one must supply information as for a CASSCF or CAS-CI calculation (e.g., choice of CAS, thresholds in Davidson diagonalization) and, in addition, (i) on the number of renormalized block states (and whether this number has been used as an upper limit or as a fixed value), (ii) the ordering of orbitals on the lattice (i.e., which orbital is to be added next to the growing system), and (iii) on the way the environment states (i.e., states defined on the complementary subset of orbitals of the CAS, the 'environment') have been treated in the first (warm-up) sweep. The role of these parameters is discussed in ref. [17]. For a tutorial demonstration of example calculations we refer to [18].

Note that there exist different variants of DMRG that refer to the number of orbitals (called 'sites' in DMRG) on which many-particle states are explicitly constructed. While usually two-site DMRG is applied in quantum chemistry, the single-site DMRG algorithm has certain advantages that may make it a good choice for certain applications. However, single-site DMRG is prone to get stuck in local energy minima (which is the reason why it is hardly applied in quantum chemistry).

While the theory behind the algorithm is very well described by Schollwoeck in [19], we may refer to [20] and [21] for presentations of the traditional (first-generation) algorithm and to ref. [22] for that of a second-generation algorithm which solely relies on the matrix-product-operator representation.

It must be emphasized that DMRG, like CASSCF, lacks dynamic correlation encoded in those orbitals that are not part of the active space. For quantitative results, these effects need to be considered. Practical solutions to this problem involve multi-reference perturbation theory [23] (and references therein), combination with (short-range) density functional theory[24], and canonical transformation theory[25].

More than a dozen reviews have been published in recent years of which we may refer to these refs. [26-29], and [30].

Electrochemistry/Cyclic Voltammetry

1. General Introduction

Electrochemistry is perhaps one of the oldest and most interdisciplinary fields of the sciences, although its breadth often means that it is hidden as the underlying wide range of topics ranging from energy, biology and biochemistry, sensors, materials science and healthcare. Electrochemistry is in itself a multidisciplinary field drawing from physics and mathematics as much as it does from chemistry. From a molecular perspective electrochemistry offers the opportunity to determine thermodynamic parameters directly through the direct relation between Gibbs energy and electrochemical potential. Furthermore it allows for changes in molecular structure that proceed or are subsequent to changes in oxidation to be probed/'read-out' with sensitivities and speed orders of magnitude greater than many other analytical and spectroscopic techniques. Dynamic electrochemistry, and especially cyclic voltammetry, is probably the most widely applied technique in the study of redox active transition metal complexes and to a lesser extent techniques such as exhaustive electrolysis and differential pulse voltammetry. The topic is covered in detail in several classic textbooks, the most famous of which is:

ELECTROCHEMICAL METHODS Fundamentals and Applications, Allen J. Bard and Larry R. Faulkner 2001, John Wiley & Sons, NY.

2. Important parameters to be reported with cyclic voltammetric data

In addition to reporting of the cyclic voltammogram itself, the conditions and experimental arrangement employed should be reported as accurately as possible in order that the data can be reanalyzed at a later stage.

Instrumental aspects: First and foremost the instrumental setup should be reported rigorously including the Instrument model number, manufacturer and software version used. In addition, the use of accessories such as a rotating disc electrode, picoamp booster, amp booster, use of a Faraday cage etc. should be noted in detail. These details are important in assessing data in terms of suspected artefacts.

Electrochemical cell: The arrangement used for the experiment should be described in detail also. These include the actual reference (e.g. silver wire, silver chloride coated silver wire, SCE, silver ion etc) electrode, counter electrode (including shape and size), and above all the working electrode(s) (including shape and size). Furthermore the shape of the electrochemical cell and the use of Luggin capillaries, glass frits should be described in detail. It is important also to report the treatment methods used to clean the electrode, especially where (electro)chemical cleaning procedures have been employed.

Sample conditions: The solvent (purity), concentration of electrolyte, concentration of analyte and, if used, the internal reference, temperature, use of purge gas (e.g., argon).

Experimental method: The manner in which the voltammograms are recorded should be noted in detail; not least whether uncompensated resistance was corrected for, the open circuit potential of the cell, initial potential, equilibration time, initial scanning direction, vertex potentials, number of cycles, scan rate, current dynamic range, stirring rate and rate of electrode rotation if applicable.

Data handling and reporting: Once the cyclic voltammogram has been recorded typically data handling procedures are carried out and if so these should be noted; including the correction to a reference electrode not actually used (i.e. a silver wire reference electrode is used together with an internal reference such as decamethylferrocene and the potential scale is afterwards adjusted to that vs SCE) and the application of a correction for iR drop. The sweep segments that are shown should be noted also (e.g., sweep 3 to 5).

Electrochemistry/Differential pulse voltammetry

The rapporteur says it will be finished soon.

One short paragraph as general description (including references to "Further reading"), plus a 1-3 page description of what are the current issues with the technique, which are limiting factors, and which kind of (technical) information is critical, what data is often overlooked, etc. etc.
PLEASE:

- include references between hashes, highlight them and preferably only DOIs, e.g. #DOI: 10.1021/ct800277a# or #C. Daul, M. Zlatar, M. Gruden-Pavlovic and M. Swart, "Application of Density Functional and Density Functional Based Ligand Field Theory to Spin States", In: Spin states in biochemistry and inorganic chemistry: Influence on Structure and Reactivity, M. Swart, M. Costas (Eds.), Wiley, 2015; Ch. 2, in press#.

Electrochemistry/Exhaustive electrolysis

The rapporteur says it will be finished soon.

One short paragraph as general description (including references to "Further reading"), plus a 1-3 page description of what are the current issues with the technique, which are limiting factors, and which kind of (technical) information is critical, what data is often overlooked, etc. etc.
PLEASE:

- include references between hashes, highlight them and preferably only DOIs, e.g. #DOI: 10.1021/ct800277a# or #C. Daul, M. Zlatar, M. Gruden-Pavlovic and M. Swart, "Application of Density Functional and Density Functional Based Ligand Field Theory to Spin States", In: Spin states in biochemistry and inorganic chemistry: Influence on Structure and Reactivity, M. Swart, M. Costas (Eds.), Wiley, 2015; Ch. 2, in press#.

Electron paramagnetic resonance

The rapporteur says it will be finished soon.

One short paragraph as general description (including references to "Further reading"), plus a 1-3 page description of what are the current issues with the technique, which are limiting factors, and which kind of (technical) information is critical, what data is often overlooked, etc. etc.
PLEASE:

• include references between hashes, highlight them and preferably only DOIs, e.g. #DOI: 10.1021/ct800277a# or #C. Daul, M. Zlatar, M. Gruden-Pavlovic and M. Swart, "Application of Density Functional and Density Functional Based Ligand Field Theory to Spin States", In: Spin states in biochemistry and inorganic chemistry: Influence on Structure and Reactivity, M. Swart, M. Costas (Eds.), Wiley, 2015; Ch. 2, in press#.

EXAFS

The rapporteur says it will be finished soon.

One short paragraph as general description (including references to “Further reading”), plus a 1-3 page description of what are the current issues with the technique, which are limiting factors, and which kind of (technical) information is critical, what data is often overlooked, etc. etc.
PLEASE:

- include references between hashes, highlight them and preferably only DOIs, e.g. #DOI: 10.1021/ct800277a# or #C. Daul, M. Zlatar, M. Gruden-Pavlovic and M. Swart, "Application of Density Functional and Density Functional Based Ligand Field Theory to Spin States", In: Spin states in biochemistry and inorganic chemistry: Influence on Structure and Reactivity, M. Swart, M. Costas (Eds.), Wiley, 2015; Ch. 2, in press#.

Infrared spectroscopy

The rapporteur says it will be finished soon.

One short paragraph as general description (including references to "Further reading"), plus a 1-3 page description of what are the current issues with the technique, which are limiting factors, and which kind of (technical) information is critical, what data is often overlooked, etc. etc.
PLEASE:

• include references between hashes, highlight them and preferably only DOIs, e.g. #DOI: 10.1021/ct800277a# or #C. Daul, M. Zlatar, M. Gruden-Pavlovic and M. Swart, "Application of Density Functional and Density Functional Based Ligand Field Theory to Spin States", In: Spin states in biochemistry and inorganic chemistry: Influence on Structure and Reactivity, M. Swart, M. Costas (Eds.), Wiley, 2015; Ch. 2, in press#.

Ligand-field Density Functional Theory

Density Functional Theory based Ligand Field model (LF-DFT)[31, 32] is non-empirical model based on a multi-determinant description of the multiplet fine structure.[33] It works by evaluating the DFT energy of all the Slater determinants arising from the d^n configuration of the transition metal ion in the environment of coordinating ligands using Kohn-Sham orbitals. This set of energies are then analyzed within a ligand-field model to obtain variationally the energy and multi-determinant wavefunction of the ground and excited states. In doing so, both dynamical correlation (via the DFT exchange-correlation energy) and non-dynamical correlation (via CI) is considered.

The key feature of this approach is the explicit treatment of near degeneracy effects (long-range correlation) using *ad hoc* configuration interaction (CI) within the active space of Kohn-Sham (KS) orbitals with dominant *d*-electron character. The calculation of the CI-matrices is based on a symmetry decomposition and/or on a ligand-field analysis of the energies of all single determinants (micro-states) calculated according to Density Functional Theory (DFT) for frozen KS-orbitals corresponding to the averaged configuration, eventually with fractional occupations, of the *d*- or *f*-orbitals. This procedure yields multiplet energies and fine structure splitting. With this procedure we have been able to calculate all customary molecular properties such as e.g. Zero Field Splitting, Zeeman interaction, Hyper-Fine Splitting, Jahn-Teller effect, magnetic exchange coupling, shielding constants, electronic structure and transitions in *f*-elements, *f-d* transitions etc, aware that its validity decreases with increasing metal–ligand covalency.[34] Since LF-DFT is rooted in LF theory itself, it deals with vertical excitations, and it is not possible to elucidate charge transfer (CT) transitions with this approach.[35]

The LF-DFT method: The first step consists of a spin-restricted DFT calculation of the average of the d^n configuration (AOC), providing an equal occupation, n/5, on each MO dominated by the d-orbitals. The Kohn-Sham orbitals, which are constructed using this AOC are best suited for a treatment in which interelectronic repulsion is, as is done in LF theory, approximated by atomic-like Racah parameters *B* and *C*. The next step consists of a spin-unrestricted calculation of the manifold of all Slater determinants (SD) originating from the d^n shell, i.e. 45, 120, 210 and 252 SD for d^2/d^8, d^3/d^7, d^4/d^6 and d^5 TM ions, respectively. The SD energies are used to determine the parameters of inter-electronic repulsion – Racah's parameters *B* and *C*, and eigenvalues, $\varepsilon_i = \langle\varphi_i|v_{LF}|\varphi_j\rangle (i = 1, 2,\ldots, 5)$ of the one-electron effective ligand-field Hamiltonian, v_{LF}, in a least-square sense. Eigenfunctions of the v_{LF}, φ_i, are in general a linear combination of *d* orbitals. Their energies, ε_i, are near to the energies of the AOC KS orbital energies, and one uses components of the corresponding AOC KS eigenvectors that correspond to the *d* functions to reconstruct the full representation of v_{LF}, that is, a one-electron 5 × 5 LF matrix $\langle d_i|v_{LF}|d_j\rangle$ Finally, these parameters are used to construct a full LF Hamiltonian which is diagonalized allowing to calculate all the multiplets of the full LF manifold by using CI. Comparing the SD energies from DFT with those calculated using the LF parameter values, it is found, for all considered cases that the LF parameterization scheme is remarkably compatible with SD energies from DFT; standard deviations between DFT-SD energies and their LF-DFT values are generally between 0.01 and 0.05 eV. [1] Current implementation relies on the Amsterdam Density Functional (ADF) code, and on set of Matlab scripts.

The model can treat systems with symmetry lower than cubic or even without any symmetry (C_1). For such a complex the LF matrix is off-diagonal with 15 independent matrix elements that needs to be determined in addition to the two Racah's parameters *B* and *C*. The LF matrix is obtained in a general form without prior assumptions, and do not depend on the experiment as such. It includes both electrostatic and covalent contributions to the ligand field. Moreover, being determined in a variational DFT-SCF procedure, it circumvents assumptions based on perturbation theory. It is particularly suited for cases of low symmetry and complex coordination geometries where the application of LFT, or AOM, is not easy because of the large number of model parameters.

Magnetic circular dichroism

The rapporteur says it will be finished soon.

One short paragraph as general description (including references to "Further reading"), plus a 1-3 page description of what are the current issues with the technique, which are limiting factors, and which kind of (technical) information is critical, what data is often overlooked, etc. etc.
PLEASE:

• include references between hashes, highlight them and preferably only DOIs, e.g. #DOI: 10.1021/ct800277a# or #C. Daul, M. Zlatar, M. Gruden-Pavlovic and M. Swart, "Application of Density Functional and Density Functional Based Ligand Field Theory to Spin States", In: Spin states in biochemistry and inorganic chemistry: Influence on Structure and Reactivity, M. Swart, M. Costas (Eds.), Wiley, 2015; Ch. 2, in press#.

Mass spectrometry

The rapporteur says it will be finished soon.

One short paragraph as general description (including references to "Further reading"), plus a 1-3 page description of what are the current issues with the technique, which are limiting factors, and which kind of (technical) information is critical, what data is often overlooked, etc. etc.
PLEASE:

- include references between hashes, highlight them and preferably only DOIs, e.g. #DOI: 10.1021/ct800277a# or #C. Daul, M. Zlatar, M. Gruden-Pavlovic and M. Swart, "Application of Density Functional and Density Functional Based Ligand Field Theory to Spin States", In: Spin states in biochemistry and inorganic chemistry: Influence on Structure and Reactivity, M. Swart, M. Costas (Eds.), Wiley, 2015; Ch. 2, in press#.

Molecular dynamics

Molecular dynamics (MD) methods aim at sampling the conformational space of a molecular system in a well defined statistical ensemble by integrating the relative equations of motion #H. J. C. Berendsen "Simulating the Physical World", Cambridge University Press, Cambridge 2007#. Following the ergodic hypothesis, the expectation values of any property of interest can be directly obtained by its time average over the sampled trajectory. In MD approaches, data from individual structures are not meaningful per se; rather, only the ensemble-averaged quantities are.

Integration of the equations of motion requires the explicit calculation of the forces acting on the nuclei; therefore, MD methods take different flavours (with different intrinsic advantages and issues) according to the ways the potential energy function is defined. MD methods may be classified into three different main classes:

1 - ab initio MD, 2 - MD with QM/MM, 3 - Classical MD.

Ab initio MD. In this approach, the forces acting on the nuclei are directly associated to the shape of the electronic wavefunction, which is parametrically dependent on the nuclear coordinates #D. Marx and J. Hutter "Ab Initio Molecular Dynamics: Basic Theory and Advanced Methods" Cambridge University Press, Cambridge 2009 # . The time evolution of the whole molecular system can be obtained following either the Car-Parrinello or Born-Oppenheimer MD schemes[36]. More complex methods that go beyond the Born-Oppenheimer approximation (Eherenfest dynamics, Path-integral MD etc) can be implemented whenever the system is initially prepared on an electronic state manifold or nuclear quantum dynamic effects cannot be disregarded. Typically, in ab initio MD, only non-adiabatic couplings are considered. The SHARC algorithm[37] can include any arbitrary coupling, for instance, non-adiabatic and spin-orbit couplings, on the same footage, to describe internal conversion and intersystem crossing, respectively. Explicit interactions with electric fields are also possible within SHARC.[38]

MD with QM/MM. Multilevel schemes are discussed elsewhere in the document. Briefly, a smaller portion of the system is described at accurate, quantum-mechanical (QM) level, and it is embedded into a larger environment, which is treated at a lower level of accuracy, typically Molecular Mechanics (MM). Pertinent to this section are additive (or "full Hamiltonian") QM/MM schemes[39], which contain a direct definition of both the QM/MM interaction energy between the QM and MM parts, and its derivatives with respect to nuclear positions. In this way, integration of the equations of motion is feasible and accurate[40].

Classical MD. In this case, the nuclear forces are obtained from an empirical mechanical potential, while the electronic states are not taken into account.

Concerning determination and characterization of spin states, the different approaches to MD pose different challenges.

First of all, it must be stressed that MD, per se, is not a technique that directly computes spin properties. Rather, it is a sampling method that aims at defining a set of molecular structures that should be then used to compute the properties of interest. Therefore, all MD methods must be coupled to another computational method that is used to derive the spin properties. This means that, whenever MD is used, the database must contain both a first set of entries pertinent to the MD method used, and a second set of entries specifying the technical details for the spin-state calculations. For this second set, the same entries, as those specified in the pertinent sections elsewhere in this document, must be present.

Intrinsic to the approach, data obtained are meaningful only if the statistical sampling of the conformational space is well converged. Therefore, proper check on the convergence of the properties of interest must be done (see for example[41]). The convergence problem is more critical for ab initio or QM/MM MD - in fact, these approaches require explicit calculation of the electronic potential energy surface and gradients. Thus, the sampling times are restricted to the order of picoseconds. Classical MD runs may also be affected by insufficient sampling, whenever statistically relevant conformational basins are separated by transition

barriers higher in energy than several kT's. In these cases, it is profitable to couple the exploration of the conformational space to enhanced sampling methodologies. In general, MD-based entries should report all basic information required to reproduce a MD run in the thermodynamic ensemble of choice -- system specifications (number of atoms, boundary conditions, MD integrator, time step, total sampling time), and thermodynamic ensemble of reference (target ensemble, target thermodynamic conditions, eventually pertinent thermostats/barostats used, with relative parameters). If enhanced sampling methods are used, it must be specified what method has been used, and provide key information for its implementation and convergence test. Other crucial information regards the sampling of the structures used for the computation of the properties of interest (number of structures used, time-window separating them). The database should contain as entry at least a relevant subset of the structures used for the computation of the spin properties.
Specific to ab initio or QM/MM MD, authors should specify the MD scheme used for the QM part (for example, Car-Parrinello, Born-Oppenheimer or else), as well as all details related to the electronic structure for MD. It may be that, to reduce the computational costs, the conformational sampling by MD is done at a lower QM level, while calculation of the properties is repeated using a more accurate QM method. In this case, entries for the QM calculations should be repeated in a separate section.
For QM/MM methods, it will be necessary to specify all technical details for the QM/MM coupling, as indicated by the specific rapport for QM/MM methods.
In case conformational sampling is achieved *by classical MD,* it is necessary to provide sufficient information about the parameterized potential used. In case of standard force fields, a reference to the literature may be sufficient. If specific parameters were developed for the system of interest, it may be required to deposit them as well.

Finally, MD based approaches provide expectation values as output; therefore, all data must be presented together with their statistical uncertainty.

Molecular mechanics

Molecular mechanics (MM) uses a classical 'ball-and-spring' approach to represent molecular structure and conformational energy. The MM potential is derived from a force field - a set of mathematical functions and their attendant parameters. The forces are computed exactly as in classical MD but MM is used for energy minimisation and has no time dependence. MM for systems containing transition metal centres present some significant challenges[42]. Spin crossover systems are even more difficult since computing relative spin state energies is clearly an electronic structure problem which conventional MM cannot handle directly. A solution to this problem is the QM/MM method outlined above and in the same spirit as QM/MM but employing a parametric ligand field (LF) term to deal with the electronic structure issues is ligand field molecular mechanics (LFMM)[43, 44] which as a part of the current action has recently been implemented into the Tinker modelling package[45] which should provide fresh impetus for developing parameter sets for spin state energetics.

In common with all parametric approaches, MM is only as good as the chosen set of potential energy terms and parameters allow. The force field (FF) is optimised using a 'suitable' training set which needs to be sufficiently diverse to cover the desired types of systems. Judging diversity can be tricky and worse still, in general only one spin state of each system is observed experimentally and the structure and relative energy of the other relies on QM methods. As described elsewhere in this document, QM has its own problems with spin state energetics so one of the important goals of the Action is to provide solid guidance on the best available QM methods with which to generate the training data for developing improved FFs.

While 'proof-of-concept' that LFMM can handle SCO systems is available, the studies are very restricted and significantly more work is required to explore transferability of the current parameters for FeN_6 complexes, as well as extending FF development to encompass other metal/ligand combinations. Hopefully, this process will be facilitated by the Tinker-LF implementation which will provide cheap access to the methodology.

At the moment, MM for spin states is quite a niche area with only a few groups actively involved. In terms of the critical information, when used for geometry optimisation, there is significant overlap between MM and QM methods. Issues which are more specific to MM in terms of reproducing other people's work are: 1) which PE expressions have been used for bond-stretching, angle-bending etc.; 2) the associated FF parameters; 3) the partial atomic charges and how the electrostatic energies have been evaluated - e.g. simple Coulomb, distance dependant Coulomb, reaction field, etc.;

Mössbauer

The rapporteur says it will be finished soon.

One short paragraph as general description (including references to "Further reading"), plus a 1-3 page description of what are the current issues with the technique, which are limiting factors, and which kind of (technical) information is critical, what data is often overlooked, etc. etc.
PLEASE:

• include references between hashes, highlight them and preferably only DOIs, e.g. #DOI: 10.1021/ct800277a# or #C. Daul, M. Zlatar, M. Gruden-Pavlovic and M. Swart, "Application of Density Functional and Density Functional Based Ligand Field Theory to Spin States", In: Spin states in biochemistry and inorganic chemistry: Influence on Structure and Reactivity, M. Swart, M. Costas (Eds.), Wiley, 2015; Ch. 2, in press#.

Multiconfigurational second-order perturbation theory (CASPT2-RASPT2-NEVPT2)

All *ab initio* LCAO-MO based wave function methods basically start from a wave function consisting of a single Slater determinant (SD) or configuration-state-function (CSF), built from MOs obtained from a Hartree-Fock (HF) calculation. In single-reference methods, this wave function is used as a reference for treating electron correlation is a single step. In MP2, second-order perturbation theory (PT2) is used for this purpose. This, however, only leads to accurate results if the HF wave function is qualitatively correct, that is in the absence of near-degeneracies or static (long-range) correlation effects (which is most often not the case in transition metal (TM) systems). In multiconfigurational PT2 methods electron correlation is instead treated in two steps. First, an extended reference wave function is constructed, with extra SDs or CSFs obtained by moving electrons from occupied to vacant orbitals. This reference wave function should include the most important correlation effects. Remaining (dynamic) correlation effects are treated in the second PT2 step. Depending on the type of zeroth-order Hamiltonian used for the PT2 step, the method is called C(R)ASPT2[46, 47] #B. O. Roos, K. Andersson, M. P. Fülscher, P.-Å. Malmqvist, L. Serrano-Andrés, K. Pierloot, M. Merchán, "Multiconfigurational Perturbation Theory: Applications in Electronic Spectroscopy", in: Advances in Chemical Physics:New Methods in Computational Quantum Mechanics, edited by I. Prigogine and S. A. Rice, Wiley, New York, 1996, Vol. 43, p. 219# or NEVPT2[48] (other alternatives such as multireference QDPT (Quasi-Degenerate Perturbation Theory) are also available[49]). In CASPT2 the zeroth-order Hamiltonian is defined in terms of effective (Fock-type) one-electron operators. The computational simplicity of this approach goes at the expense of (small but systematic) errors and the introduction of intruder states. Both problems have been efficiently remedied by introducing a range of shifts to the diagonal elements of the effective Fock matrix (the imaginary level shift[50] and the so-called IPEA shift ε[51], with ε= 0.25 a.u. being the standard for the C(R)ASPT2 implementation in the MOLCAS software). In NEVPT2, two-electron terms are introduced into the zeroth-order Hamiltonian, giving a conceptually more elegant but computationally more expensive method.

It is important to realize that the accuracy to be obtained from the PT2 treatment critically depends on the quality of the zeroth-order wave function, i.e. on its ability to remove the non-dynamic correlation. The most straightforward way of improving the zeroth-order approximation of the wave function (with respect to HF) is to use the CASSCF model[52]. Here, the reference wave function is constructed from all possible electronic configurations (full CI) of a selected number of “active” electrons in a selection of molecular MOs, i.e. a “complete active space” = CAS. The active space should include all MOs involved in important correlation effects. This may not always be possible, as the computational expense of CASSCF calculations increases very steeply (factorially, i.e. exponentially) with the size of the active space. At present, the maximum size of the active space that can be used in CASSCF is 16-18 electrons in 16-18 spatial orbitals (depending on the symmetry point group). In RASSCF (R standing for ‘restricted’) the full CI treatment in the active space is replaced with a more limited CI, by placing restrictions on the occupations of orbitals, which enables active spaces of thirty orbitals and more.[53]

Because of their (often) high multiconfigurational character, multiconfigurational second-order perturbation theory methods are ideally suited for electronic structure calculations on transition metal complexes. Guidelines for constructing the active space are available in the literature[47] #K. Pierloot, "Nondynamic Correlation Effects in Transition Metal Compounds" in: Computational Organometallic Chemistry, edited by T. R. Cundari, Dekker, New York, 2001#, #DOI: 10.1080/00268970310001093 56#, #DOI:10.1002/qua.23068#. As a general rule, the following MOs should be included: the metal d orbitals, ligand orbitals involved in covalent interactions with the metal d orbitals, and, at least in case of a more-than-half-filled d shell, a second set of - nominally empty- d orbitals. This then adds up to around 15 active orbitals, well suited for CASPT2 or NEVPT2. However, cases where more active orbitals are easily found[54]: complexes containing more than one metal[47] or haem and heam-related systems containing metals in high formal oxidation states[55-58]. In those cases the extension to RASPT2 (or DMRG-PT2 as a very promising alternative, see the section on DMRG) has been found to be of crucial importance for obtaining accurate results. Ample applications of CASPT2 for transition metal complexes are available in the literature, while

RASPT2 and NEVPT2 applications are so far more limited. The size of the systems that are accessible for PT2 methods has drastically increased in recent years (mainly due to the availability of RI and CD approaches for the electron repulsion integral matrix[59] and the parallel implementation of CASPT2[60]). At present, single-point calculations on molecules containing up to 80-100 atoms (~2000 basis functions) have become possible. Full structures optimizations on transition metal complexes are, however, presently out of reach. C(R)ASPT2/NEVPT2 calculations are therefore most often performed on structures obtained from DFT or from experiment.

It should be stressed that the description of spin state energetics in transition metal complexes by means of traditional wave function methods is essentially a dynamic correlation problem. By including Fermi but not Coulomb correlation, the HF wave function is extremely biased towards high-spin states (with errors of around 50 kcal/mol for *eg* the HS-LS splitting in Fe(II) complexes[61]). This bias can be reduced significantly but never be lifted by a C(R)ASSCF treatment. For a quantitative description of relative energies of different spin states, dynamic correlation needs to be considered in a second step. This then also means that extended basis sets (of at least TZVP quality), are required for obtaining accurate results. The fact that second-order perturbation theory is used for the dynamic correlation step puts a limit on the accuracy that may be expected from the methods presented here. In fact, several studies have indicated that CASPT2 (with a 'normal' active space) still tends to overstabilize HS with respect to LS states, with remaining errors in the order of 5-8 kcal/mol[57, 62, 63]. Obviously, this error could be reduced by treating a larger fraction of the correlation already at the zeroth-order level, i.e. by increasing the size of the active space. This is, however, outside the computational limits of present computational hard/software.

Multi-reference CI/Difference-dedicated CI

The rapporteur says it will be finished soon.

One short paragraph as general description (including references to “Further reading”), plus a 1-3 page description of what are the current issues with the technique, which are limiting factors, and which kind of (technical) information is critical, what data is often overlooked, etc. etc.
PLEASE:

• include references between hashes, highlight them and preferably only DOIs, e.g. #DOI: 10.1021/ct800277a# or #C. Daul, M. Zlatar, M. Gruden-Pavlovic and M. Swart, "Application of Density Functional and Density Functional Based Ligand Field Theory to Spin States", In: Spin states in biochemistry and inorganic chemistry: Influence on Structure and Reactivity, M. Swart, M. Costas (Eds.), Wiley, 2015; Ch. 2, in press#.

NMR

Atomic nuclei with odd numbers of protons or of neutrons absorb electromagnetic radiation when placed in a strong magnetic field giving rise to the phenomenon of Nuclear Magnetic Resonance. The magnetic nuclei behave as magnetic dipoles and the frequency of the radiation being absorbed depends on the strength of the magnetic field, the chemical nature of the nucleus and the chemical environment surrounding the nucleus.
The impressive power of NMR spectroscopy as a method capable of probing the structure function and dynamics of materials at atomic level derives from the discrimination among nuclei of the same nature in different chemical environments. This chemical shift arises from magnetic shielding caused by the chemical environment around a nucleus. The chemical environment around the nucleus also influences its spectroscopic behavior via scalar (through bond) or dipolar (through space) coupling with other magnetic dipoles, which can be nuclei or electrons. It also determines how longitudinal (spin-lattice) and transverse (spin-spin) magnetization relaxes away after excitation by absorption of radiation #ISBN :9780444563514#.

These aspects can all be manipulated experimentally to give origin to the myriad of applications of NMR spectroscopy in solids, liquids and gases. NMR spectroscopy is a non destructive method, given that the radiation used is typically in the radiofrequency range, is quantitative, but is relatively insensitive due to the small population difference between states with such a small energy gap. As a consequence, in modern NMR spectrometers experimental data are collected in the time domain, and several repetitions, called scans for historical reasons, are added up to improve the S/N ratio. Fourier transformation of these data yields the spectrum in frequency scale # ISBN: 978-0-470-74609-7#.
The NMR experiment can be set up in ways that the signals of a nucleus are modulated in time by the influence of other nuclei. Each of these time modulations can be Fourier transformed originating a multidimensional spectrum that provides further dispersion of the signals, and reveals correlations between interacting nuclei.
In the solid state, the molecules stay in fixed orientations relative to the applied field and therefore NMR signals assume the shape of a 'powder spectrum'. This spans several thousands of Hz with dipolar interactions being a major factor contributing to broadening the spectra of solid samples. To obviate this effect, solid state-NMR experiments are typically performed with the sample rotating around an axis aligned with the so-called magic angle to eliminate dipolar interactions and leaving sharper signals # DOI: 10.5643/9781606503522#.
Of particular relevance to the community dealing with spin-states is the fact that unpaired electrons are very strong magnets. When the magnetic susceptibility is not isotropic, the presence of the unpaired electrons causes the so-called hyperfine shifts in the signals' positions. These can arise from Fermi contact coupling or from dipolar, also called pseudocontact, coupling. Additionally, irrespectively of the anisotropy of the magnetic susceptibility, unpaired electrons enhance nuclear relaxation leading to spectral broadening. In most cases, the control of the spin-states prevents the use of metal substitution to obtain molecules of more convenient spectral characteristics, or changes in temperature to manipulate the paramagnetic effects. When adequate proton spectra cannot be obtained, using different static field strength or the use of direct detection of other nuclei with lower gyromagnetic ratio such as ^{13}C or ^{15}N may provide practical data # ISBN: 978-0-444-20529-2# .
The scientific community using NMR for chemical and bio-molecular research has over the years prepared recommendations on best practices of reporting, archiving and porting MR data[64-67]. The recommendations below are in line with those previous works.

Photophysical and photochemical methods

1. Introduction

Photochemical and photophysical methods provide insights into the properties of electronically excited states. These states are accessed when a molecule in its ground state absorbs a photon of a suitable energy (resonance condition) in the UV-visible region of the EM spectrum. Excited states are transient, as they deactivate over short timescale (typically in the ns range) to regenerate the ground state, both via radiative (luminescence) and/or non-radiative photophysical processes, or via photochemical reactions. An excited state can be considered as a new chemical species - with a n electronic distribution that is different from that of the same molecule in the ground state, and is much more reactive as a result of its higher energy content.

As excited states are generated typically by absorption of light, a first step in a photophysical/photochemical study is to record the *UV-visible absorption* spectrum (see UV-Vis section) of the target molecule in order to determine its electronic transitions. *Steady-state emission spectroscopy*, performed with a spectrofluorimeter, is the routine technique to investigate light-emitting excited states. A schematic view of a spectrofluorimeter is shown in Figure 1. A first monochromator (excitation monochromator) selects one wavelength from the source (commonly a Xenon lamp) for sample excitation. The intensity of light emitted from the sample containing the fluorophore is selected by a second monochromator and is detected by a photomultiplier. The emission monochromator and the detector are typically placed at 90° with respect to the exciting beam in order to minimize the amount of scattered exciting light that reaches the detector. However, it should be noted that any angle can be used for detection or in the case of integrating spheres, all light can be gathered. Both emission and excitation spectra can be recorded with a standard spectrofluorimeter. An emission spectrum is the wavelength distribution of emission intensity measured at a single excitation wavelength, while excitation spectra show the dependence of emission intensity, measured at a single emission wavelength, upon scanning the excitation wavelength. Emission spectra provide information about the nature of the excited state and can be used to estimate its energy. Under suitable conditions, luminescence quantum yields, *i.e.* the ratio between the number of emitted and absorbed photons, can be determined by emission spectroscopy. Quantum yields below 1 are the result of competitive deactivation of the excited state through non-radiative pathways (internal conversion, energy or electron transfer, etc.). When the excited state is deactivated (or "quenched") by interaction with another molecular species, the corresponding quenching rate constant can be determined from emission spectra (Stern-Volmer experiment). Finally, as emission intensity can be correlated to the concentration of the luminescent sample, emission spectra can also be used for analytical purposes. Generally, the excitation spectrum of a fluorophore should be superimposable onto the corresponding absorption spectrum (provided the spectrum has been recorded on a spectrometer which has been corrected for instrument response): this is useful to confirm (or not) that the corresponding emission band can be assigned to the target molecule, and not to impurities. In other cases, excitation spectra can provide information about resonance energy transfer processes. Time-resolved measurements contain more information compared to steady-state luminescence data. Lifetimes of luminescent excited states can be accessed by *time-domain measurements*, in which luminescence (that is proportional to the number of excited states present in the sample) is monitored as a function of time. Basically, the sample is excited with a light pulse (typically from a pulsed laser), the pulse width being much shorter than the decay time of the excited state; the time-dependent luminescence intensity I(t) is then measured, and the excitation-emission cycles is generally repeated to improve signal to noise levels; finally the lifetime is determined by fitting the obtained kinetic profile. In simple cases, I(t) decays following an exponential law, in agreement with a first-order kinetics, but more complex mechanisms are possible (multiexponential or nonexponential decays). When a similar instrumental setup is coupled with a continuous lamp irradiating the sample at 90° with respect to the pulsed laser, *transient-absorption spectroscopy* measurements can be performed, in which the absorption spectra of transient species generated in a short timescale after excitation of the sample are recorded.

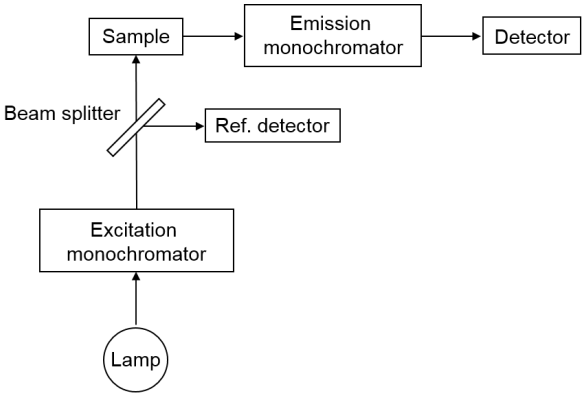

Figure 1

The topic is covered in detail in several textbooks, such the following ones:

#"Photochemistry and Photophysics – Concepts, Research, Applications", V. Balzani, P. Ceroni, A. Juris, 2014, Wiley-VCH#
#"Principles of Fluorescence Spectroscopy", Joseph R. Lakowicz, 2006, Springer#
#"Handbook of photochemistry", 3rd Ed. Marco Montalti, Alberto Credi, Luca Prodi, M. Teresa Gandolfi, CRC press#

2. Current issues

A first general consideration is that, in a typical photophysical/photochemical analysis, data should be collected in the following order: absorption spectrum, emission spectrum, excitation spectrum, time-dependent emission. Issues concerning steady-state absorption spectroscopy are discussed in the UV-Visible section. It should be only pointed out that, for an accurate determination of molar absorptivities, absorption spectra should be recorded on three or more replicates, *i.e.* on independently prepared samples, providing an "averaged ε" *vs* wavelength plot.

Regarding steady-state emission spectroscopy measurements, the following issues should be taken into account:

Instrumental aspects: the geometrical arrangement of the sample should be adapted to the nature of the sample itself. The front surface of the cuvette should be oriented at 90° or 30° with respect to the excitation beam for dilute solutions or for concentrate solutions/solids, respectively, in order to maximize the detected emission intensity.

Sample preparation:

i) Purging the sample solution with Ar or N_2 to remove triplet O_2, which acts as a quencher for triplet excited states, can be necessary (depending on the type of sample) for quantitative measurements, even if it is generally not required for qualitative studies.

ii) The sample solution should be filtered in order to remove suspended particles that could result in undesired scattering of the exciting light towards the emission monochromator.

iii) Optically dilute solution, *i.e.* solutions with absorbance less than 0.1 in the spectral region of interest (both at the wavelength of excitation and the wavelength range of emission), must be used for quantitative luminescence analyses (determination of luminescence quantum yield or Stern-Volmer rate constants). Solutions with A = 0.05 should be prepared for determination of sample concentration from emission data.

Experimental method:

i) Excitation wavelength for emission spectra should be chosen based on the absorption bands in the UV-Visible spectrum. The wavelength chosen should preferably be such that the absorption is relatively uniform over +/- 10 nm and care should be taken to use an appropriate longpass filter in the emission channel to remove scattered excitation light that appears at double the excitation wavelength (2nd order diffraction by the grating). In addition to Rayleigh scattering of the exciting beam by sample and cuvette, Raman scattering of the exciting beam by the solvent should be considered also. The presence of these spectral features can also affect excitation spectra. Again the use of cut-off or pass-band filters in front of the excitation and/or the emission monochromators is generally helpful to circumvent these interferences.

ii) Emission and excitation spectra should be corrected, as a consequence of wavelength-dependent response of the lamp, the monochromators and the detector. Thus, uncorrected spectra should be multiplied

for a correction curve. The most convenient method to obtain a correction curve is by registering the spectrum of a standard compound and comparing it with the corresponding corrected spectrum reported in the literature. It should be noted that corrections can affect the position of band maxima and band shapes in the emission spectrum.

iii) For quantitative emission measurements (concentration, quantum yield, quenching rate constants, etc.), all spectra must be recorded with the same instrumental parameters (excitation wavelength, excitation and emission slit widths, emission spectral range, etc.).

iv) For luminescence quantum yield determination, comparison with a standard compound with known quantum yield is usually required. The standard compound must emit in the same spectral range of the sample, and both sample and standard luminescence spectra must be obtained by exciting at the same wavelength.

v) Concerning Stern-Volmer experiments, excitation and emission wavelengths should be chosen, if possible, to avoid direct absorption by the quencher. Otherwise, suitable corrections of intensities must be applied.

Regarding time-resolved luminescence measurements, the main factors that should be considered are the following:

Sample preparation:

i) Dilute solution should be used.

ii) Removal of dioxygen from the solution sample is imperative when triplet excited states are involved.

Instrumental aspects and experimental method:

i) The fluorophore should absorb light at the excitation wavelength of the pulsed laser source.

ii) Excitation pulse duration of the laser should be much shorter than the lifetime to be determined.

iii) The time between two consecutive pulses (*i.e.* the inverse of the repetition rate of the light pulse) should be at least four times the longest emission decay time in the sample.

QM/MM, Multi-level schemes

When calculating the electronic properties of very large systems, for example aiming at including environmental effects of a solvent or a protein surrounding, the entire system may be split in a quantum mechanical (QM) and a molecular mechanical (MM) subregion.
The general idea is to divide the system into separate regions, which are treated at different levels of detail. The active site of an enzyme or the probe in solution and eventually the closest interacting particles are treated explicitly by QM. The nearest neighbors (amino acid residues in a biomolecular protein matrix) and surrounding solvent molecules are consequently treated at a more efficient level of computation, such as a force-field (molecular mechanics, and/or a dielectric continuum).

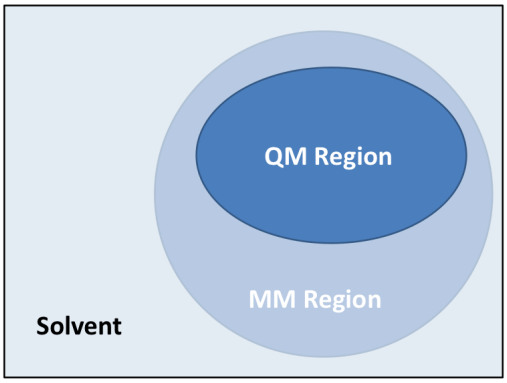

Figure 1 QM/MM *separation of the entire system into a quantum-mechanically treated subregion (QM) which is surrounded by a force field based (MM) subregion. The solvent environment can implicitly or explicitly be considered.*

Further reading

#A.Warshel and M. Levitt, Theoretical studies of enzymic reactions -dielectric, electrostatic and steric stabilization of carbonium-ion in reaction of lysozyme, *J Mol Biol*. **103**, 227–249 (1976).#
#J. Gao, Methods and applications of combined quantum mechanical and molecular mechanical potentials, *Rev. Comput. Chem*. **7**, 119–185 (1996)#
#M. J. Field, Simulating enzyme reactions: challenges and perspectives *J. Comput. Chem*. **23**, 48–58 (2002)#
#J. Tomasi, B.Mennucci and R. Cammi, Quantum mechanical continuum solvation models, *Chem. Rev*. **105**, 2999–3093 (2005)#
#H. Lin and D. Truhlar, QM/MM: what have we learned, where are we, and where do we go from here?, *Theor.Chem. Acc*. **117**, 185–199 (2007)#
#H. M. Senn and W. Thiel, QM/MM studies of enzymes, *Curr. Opin. Chem. Biol*. **11**, 182–187 (2007)#
#H. M. Senn and W. Thiel, QM/MM methods for biomolecular systems, *Angew. Chem.-Int. Ed*. **48**, 1198–1229 (2009)#

Current issues, limiting factors, (technical) information is critical. Often overlooked 1-3 pages.

State-of-the-Art in QM/MM

Over the last 10-15 years numerous reviews have documented the development of QM/MM approaches as well as their applications to biomolecular systems. The development of computing resources was critical to the advancement of QM/MM methods. The reader is referred to selected reviews by Field[1], Mulholland [2,3], Friesner [4] and Thiel [5] and Senn and Thiel [6, 7, 8] for a coverage of methods and applications.

Choice of Embedding Scheme

When QM and force field methods are combined, they are usually referred to as QM/MM methods. There are different options as to the linking and interaction of the QM and MM subregions ('embedding'). In general, one discriminates between two different embedding schemes.

In the 'electrostatic embedding' scheme the energy of the total system is then expressed as

$$E^{\text{QM/MM-EE}} = E^{\Phi,\,\text{QM}} + E^{MM} + E^{\text{QM-MM}}$$

where $E^{\Phi,\text{QM}}$ is the QM energy in the presence of field Φ generated by the partial charges of the MM region. E^{MM} is the force field energy of the MM region with all bonded and non-bonded interactions of particles in that region. $E^{\text{QM-MM}}$ describes the interaction between the two separate regions and has all force field-based 'region crossing' terms that involve QM and MM centers plus all MM van der Waals terms between one QM and one MM center. Note, $E^{\text{QM-MM}}$ does not have electrostatic interactions between QM and MM region, since those are already included in the $E^{\Phi,\text{QM}}$ part.

In the 'mechanical embedding' scheme the total energy of the system is expressed as

$$E^{\text{QM/MM-ME}} = E^{\text{QM}} + E^{MM} + E^{\text{Q, QM-MM}}.$$

The difference to the 'electrostatic embedding' is that here E^{QM} does no longer include potentials from the MM region. Instead $E^{\text{Q,QM-MM}}$ contains the calculated classical electrostatic interaction from assigned partial charges to the QM atoms and uses the force field approach to calculate point charge interactions.

The key difference between a 'mechanical' and an 'electrostatic' embedding scheme is the treatment of electrostatic interactions between the QM and MM regions. A mechanical embedding scheme handles this interaction at the MM level. This is simpler but has also disadvantages (see Table 1) since the atomic charges are sometimes difficult to obtain. Another drawback is the overpolarization of the QM region by the MM atoms. This alters the charge distribution in the QM region. When the QM reaction is accompanied by charge transfer and/or several electronic states are close in energy, this may have profound effects. In such cases, the polarization may change the energetic ordering of spin states and predict a different ground state with a different charge and spin distribution (see below).

In the ONIOM modified algorithm of electrostatic embedding [9], a *subtractive* energy expression is used

$$E^{QM/\,MM-ONIOM} = E^{MM,total} + E^{QM(QM)} - E^{MM(QM)}$$

with $E^{\text{MM,total}}$ the energy of the total system and $E^{\text{MM(QM)}}$ the energy of the QM region as calculated by the MM method. In the subtractive approach, the active site region is modeled at the MM level, and the choice of suitable MM parameters (e.g., atomic charges) for all states of the enzymatic system is an important consideration.

Table 1 **Comparison of two most QM/MM embedding schemes.**

	Electrostatic Embedding (EE)	Mechanical Embedding (ME)
Hamiltonian	$E^{\text{QM/MM-EE}} = E^{\Phi,\text{ QM}} + E^{MM} + E^{\text{QM-MM}}$	$E^{\text{QM/MM-ME}} = E^{\text{QM}} + E^{MM} + E^{\text{Q, QM-MM}}$
Advantages	Polarization of wavefunction by MM region. More accurate description of electrostatic interaction between QM and MM regions. No MM parameters for QM atoms required.	Simplified expression and implementation.
Disadvantages	Full inclusion of partial charges may lead to overestimation of electrostatic interactions. Appropriateness of MM point charges as a background of atom-centered point charges in QM region questionable. In most EE implementations, MM region not polarized by QM atoms. Computationally more demanding.	MM point charges required for both QM and MM atoms. Perturbation of QM region due to electrostatic interaction between QM and MM atoms ignored.

Terminating and Linking QM and MM Regions

The choice and definition of the quantum mechanical regional and its interaction and link with the MM part are the most critical issues.

When a covalent bond crosses the boundary region of the QM and MM parts between atoms QM_1 and MM_1, this bond is formally broken and the dangling bond has to be saturated by a link atom ('X', usually a hydrogen atom or a specially parameterized atom). Sometimes, boundary-atoms replacing MM_1 are introduced that appear in both the QM and MM calculation and mimic the cut bond.

Alternatively, a localized orbital may be placed to cap the QM region which is then kept frozen during the QM/MM calculation. The strictly localized bond orbitals (SLBOs) are determined from calculations on small cluster models and are assumed to be transferable. In the generalized hybrid orbital (GHO) approach, each MM_1 boundary atom carries four sp^3 hybrid orbitals of which only the one directed to the QM_1 atom (the 'active' orbital) participates in the SCF optimizations. The other three ('auxialliary orbitals) remain constant.

Choice of QM Level

The choice of QM method is crucial in QM/MM hybrid calculations: the method should be suitable for the computation of the parameters of interest as well as computationally feasible for the type of simulation required. Different QM methods exist, ranging from fast, semi-empirical methods (e.g., AM1, PM3, SCC-DFTB) to more accurate density functional (e.g., B3LYP) and finally molecular orbital *ab initio* (e.g., MP2, coupled-cluster) methods. Not all methods are applicable to all systems, either for reasons of accuracy, system size, or lack of parameters (e.g., for semi-empirical methods). Generally, improved accuracy comes at the price of increased calculation expense. It is possible, however, to re-parameterize approximate methods, or to apply simple corrections for specific reactions or systems; this can provide accurate methods for applications that require many energy evaluations, such as molecular dynamics simulations. Correlated *ab initio* QM methods are useful in testing the accuracy of less computationally demanding QM methods (e.g., semiempirical, or density functional theory, DFT).

Choice of MM Forcefield

The MM force field employed in a QM/MM study should be chosen such that it accurately describes the part of the system outside the QM region *and* its interactions with the QM region. For proteins, standard all-atom

force fields such as CHARMM27, AMBER ff99 or ff99SB, and OPLS-AA are commonly used. The decision as to which atoms to include in the QM region is critical, how to treat covalent bonds that cross the QM/MM boundary, determination of protonation states of residues, and how long-range electrostatic interactions are treated. It is important to test the influence of such choices on the results in order to draw reliable conclusions.
A direct comparison between different types of force fields is difficult since they were all derived and parameterized to reproduce specific structural and/or thermodynamic properties. The performance of Amber, CHARMM22 and Gromos96 variants and OPLS-AA were recently compared in terms of conformational sampling of blocked glycine and alanine dipeptides[10],[11]. The conformational space explored by different force fields was very different and rendered a direct comparison between them almost impossible. They also deviated from DFTB/MM simulations and a statistical analysis of high resolution protein crystal structures. All force fields were also shown to perform very differently with respect to a number of properties of tri-alanine compared with NMR and infrared observables [12].

Size of QM vs. QM/MM regions

During the last twenty years, QM calculations for large systems have become available. When a smaller part of a macromolecule is extracted, maybe the active site and a few nearby residues (30-300 atoms usually), the entire system can be investigated by approximate QM calculations. It appears to be sometimes necessary to fix a certain number of atoms in this QM system (e.g. the backbone Cα atoms of amino acids) and treat the rest of the protein as a continuum with a uniform dielectric constant.

QM/MM calculations on the other hand, treat a similar QM region by the same method as the QM-only calculations and, in addition, the outer region of the protein and solvent molecules are explicitly treated by MM force fields. There are only few direct comparisons between QM-only and QM/MM approaches. Which approach gives more accurate results and how do QM-only and QM/MM calculations converge with respect to the QM site?

More computationally demanding is to perform a systematic study of the convergence of QM/MM results with respect to the chosen size of the QM region [13, 14, 15, 16, 17, 18, 19, 20].
Within this context, two recent studies have demonstrated that the convergence to the 'full QM limit' is faster when using combined QM/MM techniques than QM methods [13, 16]. These studies apply increasing QM regions up to 1600 atoms and compare the results of QM/MM calculations with those of QM-only of the same region. Besides the faster convergence of QM/MM methods, both studies also agree in the necessity of applying large QM regions for a quantitative accurate result. Qualitative results, however, might be obtained at the QM/MM level of theory (not necessarily when only applying a QM model) for smaller regions. The requisite for applying large QM regions is quite intriguing. The authors denote the need of including a minimum of 300 atoms in the QM region for accuracies of ~2 kJ/mol. Of course, this accuracy refers to comparison of a QM/MM model to a 'full QM' study (of the entire system combining the MM and QM regions). This error should be added to the intrinsic QM error from the method and basis set.

Both QM cluster model and also QM/MM calculations are also very sensitive to the number of added residues to the QM region and the criteria on which their selection is based upon. [15, 21]

Recently, the convergence of QM/MM energetics with respect to a full QM-only calculation on a 446 atom system was systematically investigated[18]. 13 different variants of QM/MM embedding including several charge redistribution schemes were evaluated. Three sources of potential errors were identified: (i) the point charge model of the MM region, (ii) the improper polarization of the QM system and the non-polarizable MM region, and (iii) the approximate treatment of electrostatic interactions in vicinity of the boundary region.
Charge redistributions may introduce large errors if the charges were close to the QM/MM boundary. The best results were obtained for a mechanical embedding scheme without any charge correction scheme and without any polarization. Still the approach gave a mean unsigned error for 40 QM regions of different sizes of ~7 kJ mol^{-1} and a maximum error of ~28 kJ mol^{-1}.

Raman and Resonance Raman spectroscopy

The rapporteur says it will be finished soon.

One short paragraph as general description (including references to "Further reading"), plus a 1-3 page description of what are the current issues with the technique, which are limiting factors, and which kind of (technical) information is critical, what data is often overlooked, etc. etc.
PLEASE:

- include references between hashes, highlight them and preferably only DOIs, e.g. #DOI: 10.1021/ct800277a# or #C. Daul, M. Zlatar, M. Gruden-Pavlovic and M. Swart, "Application of Density Functional and Density Functional Based Ligand Field Theory to Spin States", In: Spin states in biochemistry and inorganic chemistry: Influence on Structure and Reactivity, M. Swart, M. Costas (Eds.), Wiley, 2015; Ch. 2, in press#.

SQUID

Principle: The number of unpaired spins in a known mass of sample and the degree of magnetic exchange between them can be accurately measured with a Superconducting Quantum Interference Device (SQUID) magnetometer at different temperatures. A typical sensitivity of $\leq 10^{-10}$ emu can be routinely attained, although higher sensitivities are also possible with specialised instruments. The spins are detected because they interfere with the current flowing across a Josephson junction superconducting loop. This gives rise to a potential difference across the Josephson junction which is proportional to the number of spins in the sample.

Instrumentation is offered by several different manufacturers with a typical maximum field strength of 7 T. The Quantum Design MPMS Evercool magnetometer is shown in Figure 1. This model incorporates helium recovery from the boil-off for compression before re-liquefaction at a cold head above the magnet.

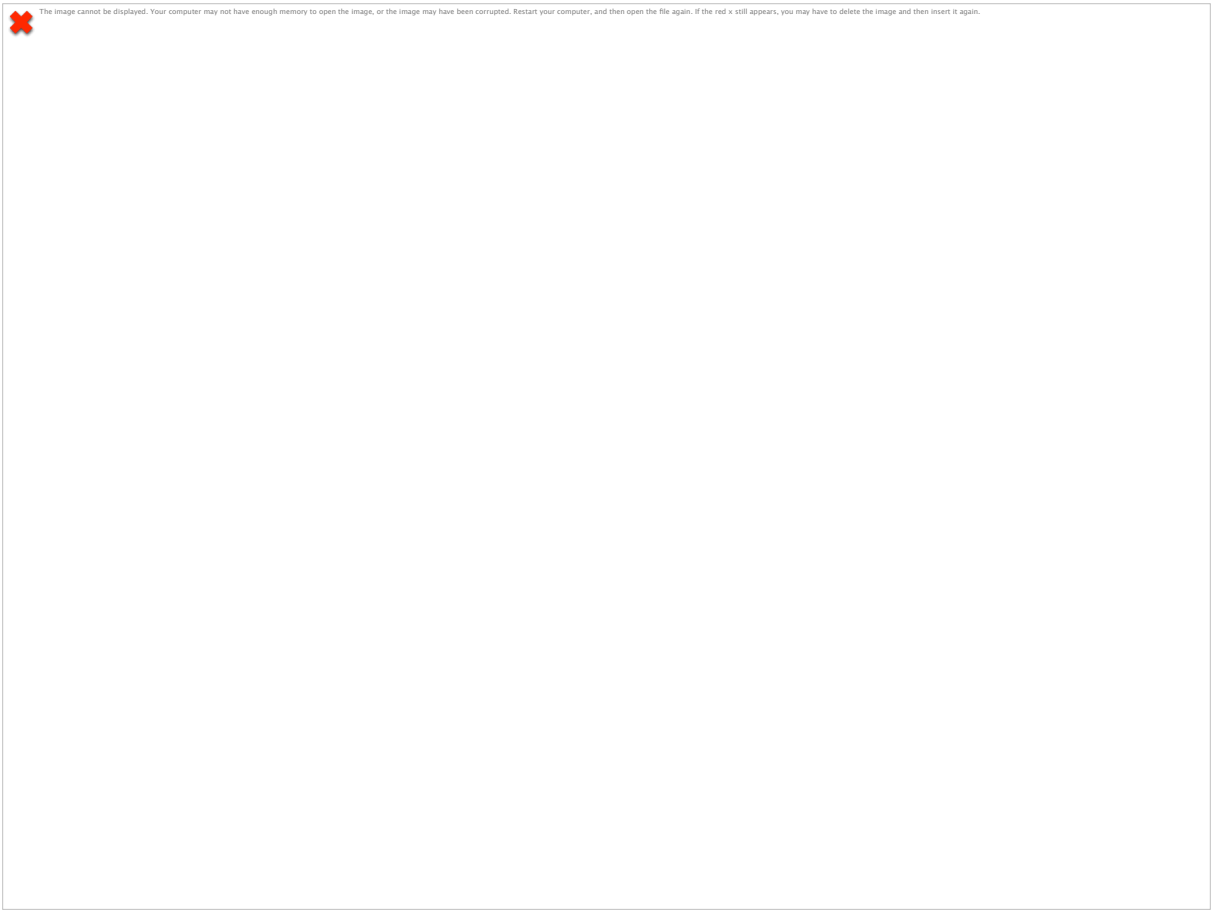

Figure 1. Quantum Design MPMS Evercool system with built-in coldhead for helium recovery.

A range of measurement temperatures are also available with the basic option to measure between liquid helium (4.2 K) and 400 K. However there are several ways to expand this temperature range including refrigeration to cool to 1.8 K or dilution with helium-3 which allows minimum temperatures of *ca*. 100 mK to be reached. There are also options to heat to 1000 K by adding a separate heating attachment although this is rarely used for molecular samples.

Stopped-flow

Stopped-flow

The stopped flow technique is an efficient method to mix chemicals in solutions and follow the fast kinetics. Single, double or triple mixing can be achieved depending on the number of syringes equipped on the apparatus. Reagents are pushed from a "reservoir syringe" to be mixed. In the stopped flow method, the mixture is pushed through a specific cuvette (scheme 1). Flow stops in the cuvette and the optical device detects the signal evolution as a function of time (signal followed can be absorbance, fluorescence, anisotropy, circular dichroism, etc.). For some examples see: [68-70]

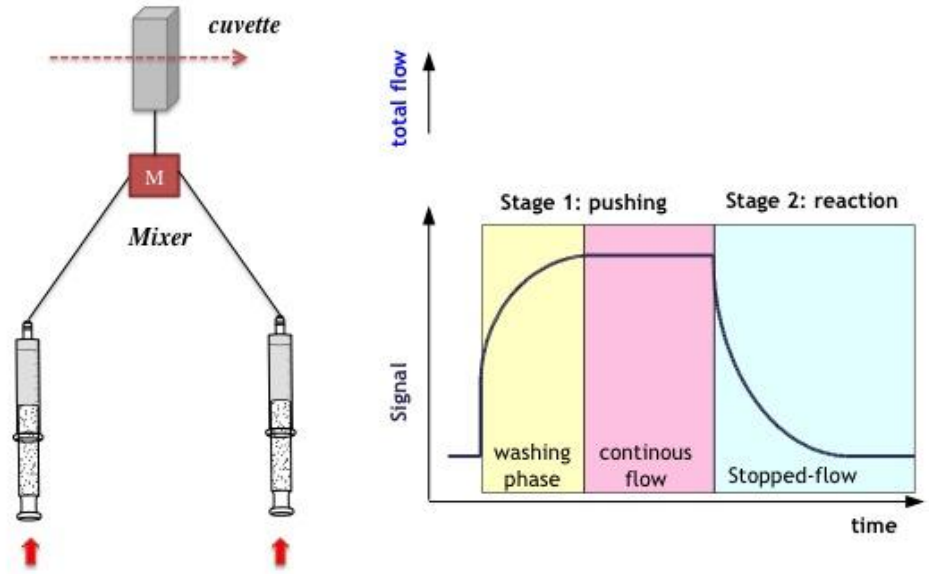

Scheme 1. Schematic representation of a stopped flow experiment.

Quench-flow or Freeze-Quench

Other useful instruments like quench flow or freeze quench allow to mix reagents and stop the reaction to trap intermediates to allow their characterization by several techniques (Scheme 2). The quench flow (chemical) allows to mix two or three samples. A quencher solution is stored in the last syringe and mixed to the pre-mixture to stop the reaction. A final and stable sample is then collected to allow its analysis using spectroscopic methods (NMR etc..).

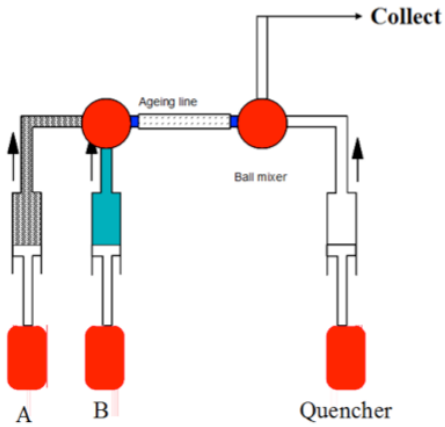

Scheme 2. Schematic representation of a Quench flow experiment.

The freeze quench allows to mix two or three samples and to age the mixture. The reaction is stopped by spraying the mixture in a cryogenic solution (generally isopentane at -120°C). The frozen sample is collected in a tube and analyzed in a second step by EPR, Mössbauer etc. For example see: [71]

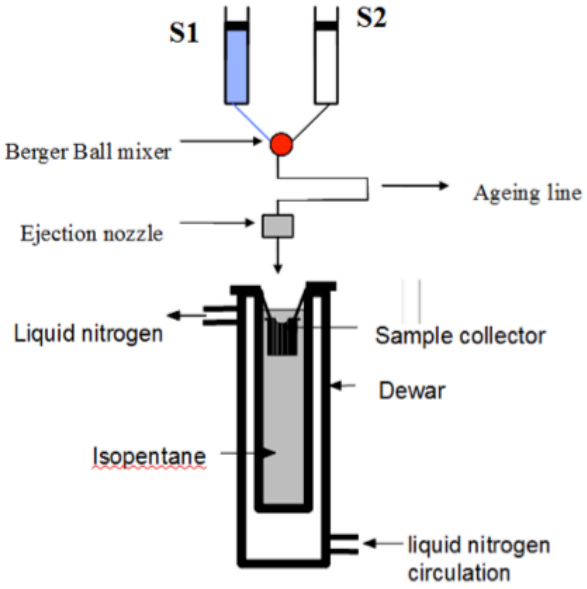

Reaction time

=

Ageing time + flying time +freezing time

Scheme 3. Schematic representation of a Freeze Quench experiment.

Time-dependent DFT

The rapporteur says it will be finished soon.

One short paragraph as general description (including references to “Further reading”), plus a 1-3 page description of what are the current issues with the technique, which are limiting factors, and which kind of (technical) information is critical, what data is often overlooked, etc. etc.
PLEASE:

- include references between hashes, highlight them and preferably only DOIs, e.g. #DOI: 10.1021/ct800277a# or #C. Daul, M. Zlatar, M. Gruden-Pavlovic and M. Swart, "Application of Density Functional and Density Functional Based Ligand Field Theory to Spin States", In: Spin states in biochemistry and inorganic chemistry: Influence on Structure and Reactivity, M. Swart, M. Costas (Eds.), Wiley, 2015; Ch. 2, in press#.

UV-Vis absorption spectroscopy

1. General introduction

UV/visible spectroscopy is a routinely used method in analytical chemistry. It analyzes the absorption features of a sample in the visible and adjacent (near-UV and near-infrared [NIR]) ranges. Although UV-Vis spectroscopy is most common for samples in solution (Figures 1a and 1b), scattering experiments (usually in a 90° angle; figure 1c) are used to investigate suspensions and solids. UV-Vis spectroscopy can be used to quantify known compounds with known absorption patterns as well as for the investigation of electronical properties of colored compounds.

In the *absorption mode* a UV-Vis spectrophotometer (Figures 1a and 1b) measures the intensity of light passing through a sample (I), and compares it to the intensity of light before it passes through the sample (I_0). The ratio I/ I_0 is called the transmittance, and is usually expressed as a percentage (%T). The absorbance, A, is then determined by the Beer–Lambert law

$A = \log(I_0/I)=\varepsilon cl$,

where ε is the molar extinction coefficient, c is the concentration of the solution, and l is the path length.

In the reflectance-mode the spectrophotometer measures the intensity of light reflected from a sample (I), and compares it to the intensity of light reflected from a reference material (I_0) (such as a white tile). The ratio is called the *reflectance*, and is usually expressed as a percentage (%R).

Different kinds of UV/Visible spectrometers are in use presently. One common kind is based on a monochromator, which separates the incident light beam into different wavelengths and the intensity of the transmitted light is measured by a photo element as a detector (figure 1a). A newer generation of spectrometer uses diode array detectors which are able to collect the whole spectra of the UV/vis region at the same moment (figure 1 b). These spectrometers are also widely used to follow reaction kinetics since it is possible to collect the whole spectra at one moment and collect multiple spectra over time. A spectrophotometer can also be either single beam or double beam. In a single beam instrument, all of the

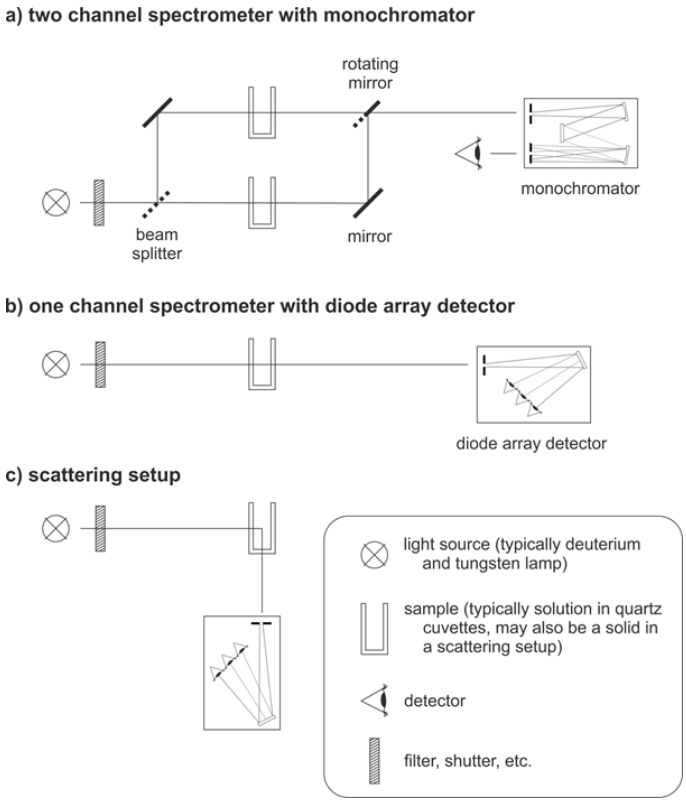

Figure 1: Several possible arrangements used commonly in UV/Vis spectrometers

light passes through the sample cell. I_0 must be measured by removing the sample. This was the earliest design and is still in common use in both teaching and industrial labs. In a double-beam instrument, the light is split into two beams before it reaches the sample. One beam is used as the reference; the other beam

passes through the sample. The reference beam intensity is taken as 100% Transmission (or 0 Absorbance), and the measurement displayed is the ratio of the two beam intensities.

2. Important parameters to report

- date
- sample description
- molecular formula
- molecular weight
- concentration (starting concentration for reactions)
- solvent / solvent mixture
- temperature
- solution stirred (yes/no)
- reaction (yes/no, for reactions followed by UV/Vis spectroscopy)
  - reactants (equivalents + solvent / volume, each)
  - reaction comments
  - spectral interval
- spectrometer
  - manufacturer
  - type
  - single- / double-beam
  - blanked for (air / empty cell / solvent / solvent mixture)
  - sample holder / cryostat
  - optics
  - shutter
  - integration time
  - wavelength (from, to)
  - resolution
- cell path length
- one full single spectra (max 2048 data points [wavelength, extinction coefficient])
- time traces (optional, up to 3 wavelength max 1023 data points + wavelength each)
- comments

References

- "Ultraviolet and Visible Molecular Absorption Spectrometry" in "Handbook of Instrumental Techniques for Analytical Chemistry", Frank A. Settle (Ed.), 1997, Prentice-Hall PTR

Vibrational circular dichroism

The rapporteur says it will be finished soon.

One short paragraph as general description (including references to “Further reading”), plus a 1-3 page description of what are the current issues with the technique, which are limiting factors, and which kind of (technical) information is critical, what data is often overlooked, etc. etc.
PLEASE:

• include references between hashes, highlight them and preferably only DOIs, e.g. #DOI: 10.1021/ct800277a# or #C. Daul, M. Zlatar, M. Gruden-Pavlovic and M. Swart, "Application of Density Functional and Density Functional Based Ligand Field Theory to Spin States", In: Spin states in biochemistry and inorganic chemistry: Influence on Structure and Reactivity, M. Swart, M. Costas (Eds.), Wiley, 2015; Ch. 2, in press#.

X-ray absorption

X-ray absorption spectroscopy (XAS) is an element selective technique, which involves the excitation of core electrons to bound states and eventually to the continuum. An XAS spectrum is typically divided into two regions: 1) the edge region, which is also referred to as the X-ray absorption near edge structure (XANES) and 2) the extended X-ray absorption fine structure region (EXAFS).

XAS edges are labeled according to the shell that the electron originates from. Therefore a 1s excitation is referred to as a K-edge and 2p or 2s excitations are referred to as L-edges. In energy of an X-ray absorption edge is sensitive to the effective charge on the absorbing atom. As the charge on the absorber increases, the energy required to remove a core electron also increase, resulting in a shift of the edge to higher energies. As such, X-ray absorption edges are frequently used as probes of oxidation state. However, it is important to keep in mind that many other factors, such as spin state, ligand identity, coordination number and site symmetry will also influence the edge energy and shape.

Beyond the edge is the so-called EXAFS region. The EXAFS region can be best understood by approximating the ejected photoelectron as a wave vector, which propagates out from the photoabsorber and may be backscattered by neighboring atoms. Due to interference between the forward propagating and backscattered electron wave vectors, an interference pattern results, which gives rise to a modulation in the absorption coefficient. By fitting the resultant modulation in the absorption coefficient, one can extract information about the identity, distance and number of backscatterers surrounding an absorbing atom.

References:

[1] DeBeer, S. and Neese, F. (2013) X-ray Spectroscopy in *Comprehensive Inorganic Chemistry (Editors: Reedijk and Poppelmeier; Publisher: Elsevier).* ***DOI:*** *10.1016/B978-0-08-097774-4.00918-9*

[2] G. Bunker, "Introduction to XAFS: A Practical Guide to X-ray Absorption Fine Structure Spectroscopy", Cambridge University Press, 2010.

X-ray emission

X-ray emission (XES) is an element selective technique which involves monitoring the fluorescence with occurs following the ionization of a core electron. When a core hole is produced on an absorbing atom, the system will relax be refilling the core hole with an electron from a higher subshell and producing a fluorescent photon. The resulting emission processes are labeled according to the subshells that are involved. For example, a 2p to 1s transition is produces a K-alpha emission line, whereas a 3p-1s transition corresponds to a K-Beta line. The K-alpha line will split into two features due to 2p spin orbit coupling and can provide some limited information about the electronic structure of the absorbing atom. In contrast, K-Beta XES is a sensitive probe of spin state in first row transition metal complexes due to 3p-3d exchange. This simple picture, however, can be strongly modulated by covalency. To higher energy one can also observe the emission which results from valence electrons refilling the 1s core hole (VtC XES). This spectral region is highly sensitive to ligand identity and metal-ligand bond distances. Due to the sensitivity of VtC XES intensities to metal-ligand bond lengths, the spectra also provide indirect information about the spin state of the system.

[1] Pollock, C. J. and DeBeer, S. (2015) Insights into the Geometric and Electronic Structure of Transition Metal Centers from Valence-to-Core X-ray Emission Spectroscopy, *Accounts of Chemical Research, ASAP,* **DOI:** 10.1021/acs.accounts.5b00309.

[2] P. Glatzel and U. Bergmann, "High resolution 1s core hole X-ray spectroscopy in 3d transition metal complexes - electronic and structural information", Coord. Chem. Rev. **249** 65-95 (2005).

3. Descriptors with information

General

Please use the following formatted table for describing the descriptors

	descriptor	*example*
1.	Molecular formula	$Fe_1C_5O_5$
2.	Total charge	0
3.	Multiplicity (assigned)	S=0
4.	Date(s) of experiments	15/09/2015
5.	General computational parameters	
5a.	Geometry optimization parameters used	
5a.1	Criterion for GradMax	1.0e-4
5a.2	Type of coordinates used	Cartesian
5b.	RHF/ROHF/UHF or RKS/UKS	
5c.	SCF parameters used	
5c.1	Mixing/damping parameter(s)	0.20 (0.15)
5c.2	Use of DIIS, ADIIS, EDIIS, etc.	DIIS
5c.3	SCF convergence criterion	1.0e-6
5c.4	Final error in [FP-PF] criterion	4.4e-7
5d.	Final value of $<S^2>$	0.0
5e.	Symmetry used	Yes
5e.1	Orbital symmetry used	D_{3h}
5e.2	Geometric symmetry used	D_{3h}
5f.	Occupation numbers for irreps	
5f.1	A'_1	26
5f.2	A'_2	2
5f.3	E'	40
5f.4	A''_1	0
5f.5	A''_2	16
5f.6	E''	12
5g.	Basis set used (for which elements)	cc-pVDZ
5g.1	Type of orbitals (GTO, STO, pw)	STO
5g.2	Frozen-core level (for ADF)	None
5g.3	Use of ECPs (for which elements)	No
5g.4	Spherical or Cartesian functions	Spherical
5g.5	Link to webpage or DOI with exponents and contraction coefficients	https://bse.pnl.gov/bse/portal
5h.	Relativistic corrections level included	Scalar-ZORA
5h.1	1-/2- or 4-component wavefunction	4-component
5h.2	Further details of the approximation	
5h.3	Nuclear model	Gaussian
5i.	Solvent effects	Yes/No
5i.1	Continuum model	COSMO
5i.1.1	Solvent, parameters	Acetone Eps=20.7 Rad=3.08
5i.2	Discrete model	polarizable embedding

5i.2.1	Charges/moments/ polarizabilities	point charges dipole moments anisotropic polarizabilities
5i.2.2	Source or algorithm	LPROP
6.	General experimental parameters	
6a.	Date(s) of experiments	15/09/2015
6b.	Phase	solution
6c.	Solvent / purity	Acetonitrile 99.8%
6d.	pH (for aqueous solutions)	7
6e.	Concentration	10^{-4} M
6f.	Temperature	298 K
6g.	Gas content (air equilibrated, N_2-purge, Ar-purge, Freeze-pump-thaw cycling)	Ar-purge

Coupled cluster/MBPT

Please use the following formatted table for describing the descriptors

	descriptor	*example*
1.	Program used	Dalton
1a.	Version	2015
1a.1	Link to download page	http://daltonprogram.org/
2.	SCF energy	45.12345678 Hartree
3.	Calculation on ground state	
3a.	Method	CCSD
3b.	Correlation energy	0.1234567 Hartree
3c.	Convergence criterion	Delta Energy = 1*10^-9
3d.	Final value of $<S^2>$	0.75
3e.	Frozen core / frozen virtuals	Yes/NO
3e.1	Window of active orbitals	5-100
3f.	Spin restriction for ROHF based methods	UCCSD
3g.	Explicitly correlated model	CCSD-F12a
3g.1	Treatment of triples correction	explicitly correlated amplitudes
3g.2	CABS corrections	Yes/NO
3g.3	Auxiliary basis set	
3h.	Local correlation model	LMO-CCSD
3h.1	Type of localization, convergence criterion	
3h.2	Cut-off parameters for domains/clusters	
3i.	Ground state property	hyperfine coupling tensor
3i.1	Detailed definition of the property	isotropic contribution for atom X
3i.2	Value of the property	70 MHz
4.	Calculation of electronically excited state	Yes/NO
4a.	Method	CCSD
4b.	Spin multiplicity	S=0
4c.	Irreducible representation	A_{2g}
4d.	Excitation energy	2.1 eV
4e.	Oscillator strength	dipole 0.123
4f.	Dominant occupied -> virtual orbital	HOMO-LUMO
5.	Calculation of second-order properties	Yes
5a.	Method	linear response CC2
5b.	Property	NMR absolute shielding
5b.1	Detailed definition of the property	isotropic contribution for atom X
5b.2	Value of the property	300 ppm
6.	Vibrational corrections	Yes
5a.	Method	VPT2
5b.	Method/basis set for force constants/ potential energy surface	CCSD(T)/cc-pVQZ
5c.	Method/basis set for property derivatives / surface	CCSD/aug-cc-pVTZ-J
5d.	Temperature	298 K
5e.	Value of the correction	1.2 Hz

DFT

Please use the following formatted table for describing the descriptors

	descriptor	*example*
1.	Program used	
1a.	Version used	
2.	Exchange-correlation used	
2a.	LDA-type exchange functional(s)	Slater
2a.1	Factors in case of composite	1.0
2b.	LDA-type correlation functional(s)	VWN
2b.1	Factors in case of composite	1.0
2c.	GGA type exchange functional(s)	PBEx
2c.1	Factors in case of composite	1.0
2d.	GGA type correlation functional(s)	PBEc
2d.1	Factors in case of composite	1.0
2e.	Global hybrid functional	No
2e.1	Percentage of global HF exchange	0.0
2f.	Range-separated hybrid functional	No
2f.1	Type of range-separation	CAM-scheme
2f.2	CAM-μ parameter	0.33 (CAM-B3LYP)
2f.3	CAM-α parameter	0.19 (CAM-B3LYP)
2f.4	CAM-β parameter	0.46 (CAM-B3LYP)
2f.1	Type of range-separation	LC-scheme
2f.2	CAM-μ parameter	0.30 (LC-PBE)
2f.3	CAM-α parameter	0.0 (LC-PBE)
2f.4	CAM-β parameter	1.0 (LC-PBE)
2f.1	Type of range-separation	LC-scheme
2f.2	CAM-μ parameter	0.30 (LC-PBE0)
2f.3	CAM-α parameter	0.25 (LC-PBE0)
2f.4	CAM-β parameter	0.75 (LC-PBE0)
2g.	Double-hybrid functional	No
2g.1	a_x parameter for HF-exchange	0.53
2g.2	a_c parameter for PT2-correlation	0.27
2h.	Dispersion energy	Grimme3
2h.1	Parameters used	Standard Grimme3
3.	Numerical integration grid type	Becke
3a.	Number of radial points/atom	590
3a.1	Radial grid type	Euler
3b.	Number of angular points/atom	99
3b.1	Angular grid type	Lebedev
3c.	Partitioning function	Becke

Density Matrix Renormalization Group

Please use the following formatted table for describing the descriptors

	descriptor	*example*
1.	Molecular formula	$Fe_1C_5O_5$
2.	Total charge	0
3.	Multiplicity (assigned)	S=0
4.	Date(s) of experiments	15/09/2015

Electrochemistry/Cyclic Voltammetry

Please use the following formatted table for describing the descriptors

	Instrumentation	*For example*
1.	Instrument manufacturer	CHInstruments
2.	model number	CHI760c
3.	Software (version)	CHI760c
4.	Picoamp booster installed	no
5.	model number of booster	N/A
6.	Faraday cage	no
7.	Electrode configuration	3 electrode
8.	reference electrode	Ag/AgCl wire
8a.	reference potential scale (i.e. corrected to...)	SCE
8a.1	luggin capillary used (yes/no)	no
8a.2	Uncompensated resistance	600 ohm
8a.3	Counter electrode	Platinum wire
8a.4	Counter electrode area	1 cm2
9.	Working electrode 1	Glassy Carbon
9a.	Working electrode shape	disc
9a.1	working electrode area	0.3 mm2
10.	Working electrode 2	none
10a.	Working electrode shape	N/A
10.a.1	working electrode area	N/A
10.a.2	Divided cell yes/no	glass frit

	Measurement conditions	*For example*
1.	Open circuit potential	0.234V
2.	Initial potential	0.2 V
3.	Equilibration time	5 s
4.	Initial scan direction	Positive
5.	Vertex potential 1	1.3 V
6.	Vertex potential 2	-.2 V
7.	Number of scan segments (typically two per cycle)	12
8.	Segments shown	3 to 5
9.	scan rate (V s-1)	0.1
10.	Current dynamic range	10-5 A
11.	iR compensation applied	yes
12.	Internal reference used	yes
13.	internal reference	decamethylferrocene
14.	conc. internal reference	0.1 mM

	Sample Conditions	*For example*
1.	Solvent	Dichloromethane
2.	Temperature	200 K
3.	Electrolyte	TBAPF6
4.	Electrolyte conc.	0.1 M
5.	Analyte concentration	1 mM
6.	Water excluded	no
7.	Analyte	vinylferrocene
8.	Purge gas	Argon
9.	Stirring	no

Electrochemistry/Differential pulse voltammetry

Please use the following formatted table for describing the descriptors

	Instrumentation	*For example*
1.	Instrument manufacturer	CHI760c
2.	model number	no
3.	Software (version)	N/A
4.	Picoamp booster installed	no
5.	model number of booster	3 electrode
6.	Faraday cage	Ag/AgCl wire
7.	Electrode configuration	SCE
8.	reference electrode	Platinum wire
8a.	reference potential scale (i.e. corrected to...)	1 cm2
9.	Counter electrode	Glassy Carbon
9a.1	Counter electrode area	disc
10.	Working electrode 1	0.3 mm2
10a.1	Working electrode shape	glass frit
10a.2	working electrode area	CHI760c
11.	Divided cell yes/no	no

	Measurement conditions	*For example*
1.	Open circuit potential	0.234V
2.	Initial potential	0.2 V
3.	Equilibration time	5 s
4.	Scan direction	Positive
5.	scan rate (V s-1)	0.001
6.	Current dynamic range	10-5 A

	Sample Conditions	*For example*
1.	Solvent	Dichloromethane
2.	Temperature	200 K
3.	Electrolyte	TBAPF6
4.	Electrolyte conc.	0.1 M
5.	Analyte concentration	1 mM
6.	Water excluded	no
7.	Purge gas	Argon
8.	Stirring	no

Electrochemistry/Exhaustive electrolysis

Please use the following formatted table for describing the descriptors

	Instrumentation	*For example*
1.	Instrument manufacturer	CHInstruments
2.	model number	CHI760c
3.	Software (version)	CHI760c
4.	Picoamp booster installed	no
5.	model number of booster	N/A
6.	Faraday cage	no
7.	Electrode configuration	3 electrode
8.	reference electrode	Ag/AgCl wire
8a.	reference potential scale (i.e. corrected to...)	SCE
8a.1	luggin cappilary used (yes/no)	no
8a.2	Uncompensated resistance	600 ohm
9.	Counter electrode	Platinum wire
9a.1	Counter electrode area	30 cm2
10.	Working electrode	Glassy Carbon
10a.	Working electrode shape	disc
10a.1	working electrode area	0.3 m2
11.	Divided cell yes/no	glass frit
	Measurement conditions	*For example*
1.	Open circuit potential	0.234V
2.	Potential	0.2 V
3.	Electrolysis time	5 s
	Sample Conditions	*For example*
1.	Solvent	Dichloromethane
2.	Temperature	200 K
3.	Electrolyte	TBAPF6
4.	Electrolyte conc.	0.1 M
5.	Analyte concentration	1 mM
6.	Water excluded	no
7.	Analyte	vinylferrocene
8.	Purge gas	Argon
9.	Stirring	no

Electron paramagnetic resonance

Please use the following formatted table for describing the descriptors

	descriptor	*example*
1.	Molecular formula	$Fe_1C_5O_5$
2.	Total charge	0
3.	Multiplicity (assigned)	S=0
4.	Date(s) of experiments	15/09/2015

EXAFS

Please use the following formatted table for describing the descriptors

	descriptor	*example*
1.	Molecular formula	$Fe_1C_5O_5$
2.	Total charge	0
3.	Multiplicity (assigned)	S=0
4.	Date(s) of experiments	15/09/2015

Infrared spectroscopy

Please use the following formatted table for describing the descriptors

	descriptor	*example*
1.	Molecular formula	$Fe_1C_5O_5$
2.	Total charge	0
3.	Multiplicity (assigned)	S=0
4.	Date(s) of experiments	15/09/2015

Ligand-field Density Functional Theory

Please use the following formatted table for describing the descriptors

	descriptor	*example*
1	General	
1.a	Program used	
1.a.1	Version used	
1.b	Geometry optimization	
1.b.1	Coordinates	file.xyz
1.b.2	Point group	O_h
1.b.3	Coordinates used from	
1.b.3.1	Geometry optimization	Yes/No
1.b.3.2	X-ray	AVEZAC(REF)
1.b.3.3	Orientation is changed	Yes/No
1.c	Charge of complex	-3
1.d	Central metal ion, d^n configuration	Cr,d3
2	DFT part	
2.a	Basis set used	TZ2P
2.a.1	Frozen-core level	none
2.a.2	indication if different for different atoms	
2.b	SCF parameters used	
2.b.1	Mixing/damping parameter(s)	0.20 (0.15)
2.b.2	Use of DIIS, ADIIS, EDIIS, etc.	DIIS
2.b.3	SCF convergence criterium	1.0e-6
2.b.4	Final error in [FP-PF] criterium	4.4e-7
2.c	Occupation for AOC	
2.c.1	A_{1g}	12
2.c.2	E_g	12 1.2
2.c.3	T_{1g}	6
2.c.4	T_{2g}	6 1.8
2.c.5	T_{1u}	6
2.c.6	T_{2u}	36
2.d	Numerical integration grid type	Becke
2.d.1	Number of radial points/atom	590
2.d.1.1	Radial grid type	Euler
2.d.2	Number of angular points/atom	99
2.d.2.1	Angular grid type	Lebedev
2.d.3	Partitioning function	Becke
2.e	Environment	Yes/No
2.e.1	COSMO: solvent, parameters	Acetone Eps=20.7 Rad=3.08
2.e.2	point charges (coordinates, charges, point group)	
2.f	Spin-Orbit	No
2.f.1	Occupation of AOC spinors	
3	LF-DFT part	
3.a	U matrix	U.txt
3.b	Energies of AOC KS MOs (in eV)	E_AOC.txt
3.c	Energies of all SD (in eV)	esd.txt
3.d	LF-matrix (and how it is obtained)	LF.txt(from fit)

3.e	Inter-electronic parameters	
3.e.1	Racah’s parameter B	3600
3.e.2	Racah’s parameter C	800
3.f	Orbital reduction factor	0.89
3.g	Spin-Orbit Coupling constant zeta	No
3.g.1	taken from literature	350(REF)
3.g.2	ionic (corrected for covalency)	320(Yes)
3.g.3	taken from 2.f.1	No
3.h	magnetic field used	No
3.i	rmsd value for the fit	92

Magnetic circular dichroism

Please use the following formatted table for describing the descriptors

	descriptor	*example*
1.	Molecular formula	$Fe_1C_5O_5$
2.	Total charge	0
3.	Multiplicity (assigned)	S=0
4.	Date(s) of experiments	15/09/2015

Mass spectrometry

Please use the following formatted table for describing the descriptors

	descriptor	*example*
1.	Molecular formula	$Fe_1C_5O_5$
2.	Total charge	0
3.	Multiplicity (assigned)	S=0
4.	Date(s) of experiments	15/09/2015

Molecular dynamics

Please use the following formatted table for describing the descriptors

	descriptor	*example*
	FOR ALL MD RUNS:	
1.	Program used	CP2K
2.	Simulated system	Azurin from P. aeruginosa
3.	Solvent	Water
3.a	Treatment of the solvent	Explicit
3.b	Solvent model (if pertinent)	TIP3P
3.b.1	Implicit solvent parameters (if pertinent)	□= 80
3.c	Boundary conditions	PBC
3.c.1	Initial cell size	10.15 x 8.32 x 7.23 nm^3
4.	System size (n. of atoms)	28645
4.a	Information on initial structure	PDB entry
4.b	Total charge of the solute system	+3 |e|
4.c	Species and number of counterions	Cl-, 3
4.d	Number of solvent molecules	7328
4.e	Initial coordinates of the system	File deposit
4.f	Side-chains in non-standard protonation state	Asp241, Glu53
5.	Type of MD	ab initio MD
6.	Timestep	1.5 fs
6.a	Total simulation time	200 ns
7.	Thermodynamic ensemble	NpT
7.a	Target thermodynamic parameters	300K, 1 atm
7.a.1	Thermostat used	Nose-Hoover
7.a.1.1	Parameters for the thermostat	1.0 ps
7.a.2	Barostats used	Berendsen
7.a.2.1	Parameters for the barostat	1.0 ps
8.	MD integrator	Leapfrog
9.	Velocity initialization random seed	160967
10.	Treatment of electrostatic interactions	PME
10.a	Parameters for electrostatics	Grid (specify)
11	Treatment of vdW forces	cutoff
11.a	Cutoff-value	1.2 nm
12	Pairlist	yes
12.a	Pairlist update	50 steps
	FOR ab-initio MD or QM/MM MD:	
1.	MD scheme for the QM part	Car Parrinello
2.	QM method	DFT
3.	All information required to define the QM calculation	See pertinent entries elsewhere
4.	QM/MM coupling scheme	Full-Hamiltonian
4.a	QM/MM parameters	See pertinent entries elsewhere
	FOR classical MD:	

1.	Force-field	Amber (specify version)
1.a	Non-standard topology file and parameters	File deposit
2.	Constraint algorithm	SHAKE
2.a	Constraint algorithm threshold	0.0001

	FOR THE CALCULATION OF THE SPIN PROPERTIES	
1.	Number of structures used	24
2.	Sampling time window	500 ps
3.	Set of structures used	File deposit
4.	Method used for calculation of spin properties	Ligand Field DFT
5.	Specifications required to perform the spin calculation	See pertinent entries elsewhere

Molecular mechanics

Please use the following formatted table for describing the descriptors

	descriptor	*example*
1.	Molecular formula	$Fe_1N_6H_{17}$
2.	Total charge	2
3.	Multiplicity (assigned)	S=2
4.	Software	DommiMOE2011
4a.	Base Force Field	MMFF94
4b	Additional FF	LFMM
4b.	FF Parameters	Deposited files
4c.	Partial charges	Deposited file
4d.	Convergence criterion	0.01 kcal/mole
5.	Optimised coordinates	Deposited file
5a	Potential energy	-125.12 kcal/mol

Mössbauer

Please use the following formatted table for describing the descriptors

	descriptor	*example*
1.	Molecular formula	$Fe_1C_5O_5$
2.	Total charge	0
3.	Multiplicity (assigned)	S=0
4.	Date(s) of experiments	15/09/2015

Multi-configurational wavefunctions

	Instrumentation	*For example*
1.	Program used	MOLCAS
1a.		8.0
1a.1		http://www.molcas.org
2.	Method used	RASPT2
3.	Structure used	provide XYZ file
3a.	Method used to obtain structure	DFT(BP86)/def2-TZVP
3b.	Coordinates	provide XYZ fie
4.	For each calculated state:	
4a.	Spin multiplicity	S=1
4b.	Symmetry representation	A2
4c.	Number of states N included in the orbital optimization	3
4c.1		1,2,4
4c.2		1,2,1
4d.	C(R)ASSCF energy	-2215.16849743
4d.	Total energy (CASPT2,NEVPT2)	-2219.84944035
5.	Details on the reference space (if different for different states, repeat this section for each state)	
5a.	Frozen orbitals ? (yes/no)	yes/NO
5a.1	If YES, frozen at which level ?	
5a.2	If YES, frozen orbitals for irreps	
5b.	Inactive orbitals for irreps	
5b.1	A1	29
5b.2	B1	22
5b.3	A2	16
5b.4	B2	22
5c.	Specification of active electrons	
5c.1	Number of active electrons = n	14
5c.2	Max number of holes in RAS1 = j	0
5c.3	Max number of of electrons in RAS3 = k	2
5d.	RAS1 orbitals for irreps, only if j¹0	
5e.	RAS2 orbitals for irreps	
5e.1	A1	4
5e.2	B1	2
5e.3	A2	3
5e.4	B2	2
5f.	RAS3 orbitals for irreps, only if k¹0	
5f.1	A1	1
5f.2	B1	3
5f.3	A2	0
5f.4	B2	2
5g.	If possible, provide a contour plot of the active orbitals	
6.	Second-order perturbation treatment	
6a.	frozen orbitals for irreps	
6a.1	A1	11
6a.2	B1	7
6a.3	A2	5
6a.4	B2	7
6b.	deleted orbitals for irreps, if any	0
6c.	For CASPT2/RASPT2: Value of IPEA-shift	0.25

	(standard = 0.25 a.u.)	
6d.	For CASPT2/RASPT2: possible information on level shift: real shift (RS) or imaginary shift (IS) = value of shift	IS=0.1
6e.	For NEVPT2: partially or strongly contracted	

Multi-reference CI/Difference dedicated CI

Please use the following formatted table for describing the descriptors

	descriptor	*example*
1.	Molecular formula	$Fe_1C_5O_5$
2.	Total charge	0
3.	Multiplicity (assigned)	S=0
4.	Date(s) of experiments	15/09/2015

NMR

	Instrumentation	*For example*
1.	Data acquisition	
1a.	Nulcei probed directly and (if any) indirectly	
1b.	identification of the standard used as reference for the chemical shift scale and referencing procedure (internal, external, ...) following the recommendations in *Pure Appl. Chem.*, Vol. 80, No. 1, pp. 59–84, 2008.	
1c.	Field	
1d.	Spectral window	
1e.	Spectral resolution	
1f.	Number of scans	
1h.	Temperature	
1i.	Nature of probe used	
1j.	Pulse program used including dimensionality, sequence, length, power and duration of pulses, and duration of delays, and frequency offsets	
1k.	Data recording methods	
1l.	Pressure if different from atmospheric	
2.	Data processing	
2a.	Software used	
2b.	Amount of zero filling	
2c.	Apodization function used	
2d.	If and what post-processing methods for solvent signal elimination were used	
2f.	If and what method of baseline correction was used	
3.	For liquid samples	
3a.	Sample preparation	
3a.1	Solvent (including the use of co-solutes or jellifying agents for mobility restriction)	
3a.2	pH (for aqueous solutions)	
3a.3	Concentration of the solute	
3a.4	Tube diameter	
3a.5	Whether oxygen was removed from the sample or a special atmosphere was user	
4.	For SS and HRMAS	
4a.	Sample preparation	
4a.1	Size of the rotor	
4a.2	Amount of sample	
4b.	Data acquisition	
4b.1	Solvent (including the use of co-solutes or jellifying agents for mobility restriction)	
4b.2	pH (for aqueous solutions)	
4b.3	Concentration of the solute	
4b.4	Tube diameter	
4b.5	Whether oxygen was removed from the sample or a special atmosphere was user	
4b.6	Rotor speed and whether a double rotor was used	

For biomolecular samples we should adhere to the recommendations in # 10.1023/A:1008290618449#. and in # doi:10.1038/nsmb.3041#

Photophysical and photochemical methods

	Instrumentation	*For example*
1.	Absorption spectroscopy	see UV-Vis section
2.	Luminescence Spectroscopy	
2a.	Sample	
2a.1	Reference compound (name, formula, l_{max} emission, reported Luminescence Quantum Yield, citation of the corresponding publication), for Luminescence Quantum Yield measurements	[Ru(bpy)3]Cl2 (F = 0.042 in H2O)
2a.2	Concentration of added quencher, for Stern-Volmer Luminescence Quenching Experiment	5.10-5 to 5.10-4 M
2b.	Instrument	
2b.1	Spectrofluorimeter (name/model, manufacturer)	Horiba FluoroMax-4
2b.2	Software and version (for data acquisition and processing)	FluorEssence v. 3.5
2b.3	Geometric arrangement (angle between the incident beam and the surface of the sample cell)	90°
2b.4	Correction (if so, how)	yes, comparison with the spectrum of a standard compound
2b.5	Optical path length	1 cm
2b.6	Source (type, static/pulsed, spectral range/wavelength)	Xenon arc lamp, continuous, 250-1000 nm
2b.7	Filter(s) type (cut-off/band-pass/interference/none)	Short-wavelength cut-off
2b.8	Filter(s) absorption spectrum/ range	450 nm (cut-off)
2b.9	Filter position	Front exit slit
2b.10	For time-resolved:	
2b.10.1	Method (Single Flash, Single-Photon Counting, etc.)	Single-Photon Counting
2b.10.2	Excitation Pulse duration (FWHM)	30 ps
2b.10.3	Number of time intervals	1000
2b.10.4	Repetition rate (= 1/time between pulses)	10 Hz
2b.10.5	Detection method (9-stage or 5-stage PMT, iCCD, Chopper etc.)	9-stage PMT
2c.	Spectral acquisition/processing parameters	
2c.1	Emission spectra:	
2c.1.1	Excitation wavelength	450 nm
2c.1.2	Excitation slit width	5 nm
2c.1.3	Emission spectral range	520-700 nm
2c.1.4	Emission slit width	5 nm
2c.2.	Excitation spectra	
2c.2.1	Excitation spectral range	250-530 nm
2c.2.2	Excitation slit width	5 nm
2c.2.3	Emission wavelength	610 nm
2c.2.4	Emission slit width	10 nm
2c.3.	Lifetimes	
2c.3.1	Excitation and emission wavelengths	455 nm, 610 nm
2c.3.2	Fitting model (software used)	Mono-exponential (FluoFit)

QM/MM, Multi-level schemes

Please use the following formatted table for describing the descriptors

QM Region

	descriptor	*example*
0.	QM code name and version	Gaussian03, Turbomole 6.6, ADF2014.01
	Operating system	Linux Ubunto
1.	Molecular formula	$Fe_1C_5O_5$
	Number of atoms in QM region	11
2.	Total charge of atoms in QM region	0
3.	Multiplicity (assigned)	S=0
4.	Date(s) of experiments	15/09/2015
5a.	Geometry optimization parameters used	
5a.1	Criterium for GradMax	1.0e-4
5a.2	Type of coordinates used	Cartesian
5b.2	Use of DIIS, ADIIS, EDIIS, etc.	DIIS
5b.3	SCF convergence criterium	1.0e-6
5b.4	Final error in [FP-PF] criterium	4.4e-7
5c.	Final value of $<S^2>$	0.0
5e.	Basis set used	
5e.1	Type of orbitals (GTO, STO, pw)	STO
5e.2	Frozen-core level (for ADF)	None
5e.3	Use of ECPs (for which elements)	No
5e.4	Spherical or Cartesian functions	Spherical
5f.	Relativistic corrections level included	Scalar-ZORA
5g.	Symmetry used	Usually C1.
5h.	Auxiliary basis set used (if applicable)	
6.	Electronic structure level	
	Semi-empirical	PM3/AM1/MNDO
	Ab initio method	HF, (L)MP2, MRCI, CASSCF, (L)CCSD(T)
	More details (if applicable)	Active space, orbitals etc.
	Density functional theory	
	Exchange correlation functional (GGA, Hybrid, meta-GGA, etc.)	BP86, PBE0, B3LYP, TPSSh
	Modified amount of Hartree-Fock exchange	10%, 15%, 25%
7.	Other	
8.	Coordinates of atoms in QM region (element symbol xyz in Å)	C 1.5 2.32 0.0 …

Additional second QM Region present?
Repeat Table input from above with the same data and information

MM Region

Pre-Treatment of System

	descriptor	*example*
0.	Starting structure	
	pdb entry ID	1R2Q
	Homology model (target Uniprot ID, template	SwissModel, Modeller

	pdb entry ID, software and alignment algorithm, sequence identity)	P35557, ClustalW 2.1, 85%
1.	Number of atoms in MM region	12253
2.	List of residues with non-standard protonation states	Glu A 64, His B 353
3.	Solvation protocol	
	Number and position of solvent molecules	HOH, pdb or xyz format
4.	Treatment of alternative side chain conformations	Only conformer A considered, B ignored.
5.	Deleted sidechains/atoms/molecules	List of entries
6.	Presence and positioning of counterions	
	Ionic strength	150 mM
	pH	7.0
7.	Minimization protocol	Algorithm, steps, convergence criteria
8.	Equilibration protocol	Algorithm, time step, convergence criteria
	Proton position relaxation, water molecules, entire system	

MD Treatment of system if applicable

Insert formatted table from MD part.
Same details as in MD white paper need to be given here.

	descriptor	*example*
1.	Software	
2.	Forcefield	
3.	Ensemble	NVT
3.	Time step, number of iterations	2 fs, 200.000
4.	Details	
4a.	Temperature (control)	
4b.	Pressure (control)	
4c.	Periodic Boundary Conditions (PBC)	
4d.	Long-range electrostatic interactions (e.g.Ewald summation)	
5.	Generation of snapshots to be used in QM/MM calculations	
	Average structure:	List of all atoms in pdb format
	Snapshots at simulation time:	List of all atoms of all snapshots in pdb format

MM Region as used in QM/MM Calculation

	descriptor	*example*
1.	Forcefield used (name and version)	CHARMMFF29
2.	Modified partial charges for atoms	Atom name, atom number, new partial charge
3.	Other modified forcefield parameters	Atom name, atom number, modified parameter
4.	Number of MM atoms used in QM/MM calculation	1200
	Coordinates of (all) atoms in pdb or xyz format	
5.	If applicable	
	Additional continuum model	PCM, COSMO, other
	Solvent dielectric constant(s)	20

QM/MM Linkage

	descriptor	*example*
1.	Name and version of software used	
2.	QM/MM energy expression	subtractive ☐, additive ☐, other ☐
	Popular name of QM/MM scheme	ONIOM ☐, 'Full Hamiltonian' ☐, other ____
3.	Electrostatic coupling between QM and MM parts	
		Mechanical ☐, electrical ☐, polarizable ☐ (polarizable point dipoles ☐, Drude oscillators ☐, fluctuating charges ☐), other ☐ _____
	In case of Electrical Embedding	Atoms for which charges were deleted, modified, or moved: (list)
	In case of Mechanical Embedding:	
	How were atomic charges calculated	CHELP, CHELPG, Merz-Kollman, RESP, …
	How often were atomic charges updated?	
4.	Long-range electrostatic QM-MM	Ewald ☐, charge scaling ☐, variational electrostatic projection ☐, generalized solvent boundary potential ☐
5.	QM-MM van-der-Waals interactions?	No./Yes. How?
6.	QM-MM boundary	
	Link atom	Placement of link atom description
	Boundary atom	Placement of boundary atom description
	Localized orbital	Placement of localized orbital description

Type of QM/MM Calculation

	descriptor	*example*
1.	Specifiy type of QM/MM calculation	
1a	Single-point	
1b.	Geometry optimization QM/MM	
1c.	Constraints/optimization of hydrogen atoms only	
1d.	QM region only optimized in MM environment	
2.	QM/MM Molecular Dynamics	
3.	Several QM/MM single point calculations	
3a.	Different snapshot structures from one MD?	How generated?
3b.	Different MD trajectories?	Different conditions, starting configurations
4.	Weighting of results	Averaged, Boltzmann-weighted

Raman and Resonance Raman spectroscopy

Please use the following formatted table for describing the descriptors

	descriptor	*example*
1.	Molecular formula	$Fe_1C_5O_5$
2.	Total charge	0
3.	Multiplicity (assigned)	S=0
4.	Date(s) of experiments	15/09/2015

	Instrumentation	*For example*
1.	Detector	CCD
2.	Model	idus-420-OE
3.	Pixel width	25 micron
4.	number of pixels (horizontal)	2000
5.	Manufacturer	ANDOR technology
6.	Spectrograph	Shamrock300i
7.	Manufacturer	ANDOR technology
8.	Grating resolution	1200 l/mm
9.	Grating blaze	500 nm
	Optical path	
1.	Free space	yes
2.	Fiber coupled	no
3.	Microscope	no
4.	Corrected response	no
5.	Slit width (spectrograph)	50 micron
	Polarisation	
1.	Polarisation (excitation, V/H)	no
2.	Polarisation (analyzer, V/H)	no
3.	Polarisation scrambler before slit?	no
	Laser	*For example*
1.	wavelength	
2.	Manufacturer	473 nm
3.	Maximum output	Cobolt
4.	Fibre coupled	100 mW
5.	Free space	No
6.	Polarisation	Yes
	Experimental settings	*For example*
1.	sample state	
2.	neat solid/Liquid/Gas	no
3.	Solution	yes
4.	analyte	[Ru(bipy)3]PF6
5.	solvent	CH3CN
6.	Concentration	1 mM
7.	Absorbance at excitation wavelength	0.2

8.	Temperature at sample	77K
9.	Temp control	yes
10.	Control method	Liq N2
11.	Sample holder	glass 5 mm NMR tube
12.	static or moving	static
13.	Laser power at sample	50 mW
	Detection	*For example*
1.	Slit width	40 micron
2.	calibration method	Acetonitrile/toluene 50/50 quadratic fit
3.	Collection arrangment	180o backscattering
4.	Laser fibre diameter	N/A
5.	collection fibre diameter	N/A
	Analysis	*For example*
1.	dark background subtraction applied	no
2.	Baseline correction	yes
3.	Baseline correction type	multipoint spline fit
4.	Solvent subtraction carried out	no

SQUID

Please use the following formatted table for describing the descriptors

	descriptor	*example*
1.	Essential	
1.a	Molecular formula, empirical and complex to explicitly show solvation.	$[ML_6]PF_6 \cdot CH_3OH$
1.b	Form of sample	solid, liquid or solution, ground or crystal, precipitated
1.b.1	If solution, concentration should be given	
1.c	Magnetic Field strength	
1.d	Temperature range	
1.e	Scan rate	
1.f	Frequency mode AC/DC	
2.	Desirable	
2.a	Manufacturer/model	
2.b	g value	
2.c	Simulation software	

Stopped-flow

	Descriptor	*example*
1.	*General Instrument parameters*	
1a.	Brand of the instrument	Biologic
1b.	Mixer	SFM 300
1c.	Detection device (spectrophotometer/ CD etc.)	MOS/200M
1d.	Software version	Biokine32
1e.	Mixer type	Berger ball
1f.	Temperature and type of temperature-control device	
2.	*General experimental parameters*	
2a.	Solvent	acetonitrile
2b.	Number of samples to be mixed	2
2c.	Samples description	Fe^{II} Complex in MeOH hydrogen peroxide in MeOH
2d.	Initial or final concentrations	2mM to 0.5mM
2e.	Mixing ratio	1:1
2f.	Flow-rate	14.0 $mL.s^{-1}$
2h.	Delay line (if applicable)	
2g.	Atmosphere control and method (if applicable)	anaerobic (glove box)
2i.	Integration time	1 ms
2j.	Time base (number of measurements / delay between them/average between them)	2490 pt / 0 /100
3.	*Analysis parameters*	
3a.	Reaction description / reaction scheme	Monitoring of B / A>B>C
3b.	Kinetic model	Pseudo-first order formation (k1) and degradation (k2)
3c.	Analytical equation	A0*(k1/(k2-k1))*(exp(-k1*x)-exp(-k2*x))+A∞+a*x
4.	*Spectrophotometric, fluorescence or circular dichroism detection*	

4a.	Type of Cuvette and Path-length	1 cm
4b.	Type of source	
4c.	Type of detector	
4d.	Wavelength	
5.	*Freeze-Quench*	
5a.	Delay	
5b.	Nozzle	
5c.	Cryogenic solution	
5d.	Sample holder	
6.	*Chemical Quench Flow*	
6a.	Quencher preparation	

Time-dependent DFT

Please use the following formatted table for describing the descriptors

	descriptor	*example*
1.	Molecular formula	$Fe_1C_5O_5$
2.	Total charge	0
3.	Multiplicity (assigned)	S=0
4.	Date(s) of experiments	15/09/2015

UV-Vis

Please use the following formatted table for describing the descriptors

	descriptor	*example*
1.	Molecular formula	$Fe_1C_5O_5$
2.	Total charge	0
3.	Multiplicity (assigned)	S=0
4.	Date(s) of experiments	15/09/2015

Vibrational circular dichroism

Please use the following formatted table for describing the descriptors

	descriptor	*example*
1.	Molecular formula	$Fe_1C_5O_5$
2.	Total charge	0
3.	Multiplicity (assigned)	S=0
4.	Date(s) of experiments	15/09/2015

X-ray absorption

Please use the following formatted table for describing the descriptors

	descriptor	*example*
1.	Date	
2.	Sample description	
3.	Molecular formula	
4.	Molecular weight	
5.	Sample state	solid, solution
6.	Sample holder	
7.	Sample thickness	
8.	Concentration	
9.	Temperature	
10.	Beam line where data were collected	
11.	Optics configuration	
12.	Detection method(s)	trans, e-yield, fluorescence, high-resolution fluorescence
13.	Calibration method	
14.	Information on damage assessment	
15.	Scanning mode	energy scan, dispersive
16.	Scan parameters used	step size, count time, energy range
17.	Number of scans	
18.	Raw ascii data with eV, I0 and raw data should be provided	
19.	For exafs, k and EXAFS, should be included	

X-ray emission

Please use the following formatted table for describing the descriptors

	descriptor	*example*
1.	Date	
2.	Sample description	
3.	Molecular formula	
4.	Molecular weight	
5.	Sample state	solid, solution
6.	Sample holder	
7.	Sample thickness	
8.	Concentration	
9.	Temperature	
10.	Beam line where data were collected	
11.	Beam line optics configuration	
12.	Analyzer optic, analyzer geometry and detector	
13.	Calibration method	
14.	Information on damage assessment	
15.	Scanning mode	energy scan, dispersive
16.	Scan parameters used	step size, count time, energy range
17.	Number of scans	
18.	Raw ascii data with eV, I0 and raw data should be provided	

The End

1. Bartlett, R. J.; Musiał, M., Coupled-cluster theory in quantum chemistry. *Reviews of Modern Physics* **2007**, 79, 291-352.
2. Krylov, A. I., Equation-of-Motion Coupled-Cluster Methods for Open-Shell and Electronically Excited Species: The Hitchhiker's Guide to Fock Space. *Annual Review of Physical Chemistry* **2008**, 59, 433-462.
3. Sneskov, K.; Christiansen, O., Excited state coupled cluster methods. *Wiley Interdisciplinary Reviews: Computational Molecular Science* **2012**, 2, 566-584.
4. Harvey, J. N., The coupled-cluster description of electronic structure: perspectives for bioinorganic chemistry. *Journal of Biological Inorganic Chemistry* **2011**, 16, 831-839.
5. Petit, A. S.; Pennifold, R. C. R.; Harvey, J. N., Electronic Structure and Formation of Simple Ferryloxo Complexes: Mechanism of the Fenton Reaction. *Inorganic Chemistry* **2014**, 53, 6473-6481.
6. Chen, H.; Lai, W.; Shaik, S., Exchange-Enhanced H-Abstraction Reactivity of High-Valent Nonheme Iron(IV)-Oxo from Coupled Cluster and Density Functional Theories. *Journal of Physical Chemistry Letters* **2010**, 1, 1533-1540.
7. Riplinger, C.; Neese, F., An efficient and near linear scaling pair natural orbital based local coupled cluster method. *Journal of Chemical Physics* **2013**, 138, 034106.
8. Kozlowski, P. M.; Kumar, M.; Piecuch, P.; Li, W.; Bauman, N. P.; Hansen, J. A.; Lodowski, P.; Jaworska, M., The Cobalt–Methyl Bond Dissociation in Methylcobalamin: New Benchmark Analysis Based on Density Functional Theory and Completely Renormalized Coupled-Cluster Calculations. *Journal of Chemical Theory and Computation* **2012**, 8, 1870-1894.
9. Neese, F.; Hansen, A.; Liakos, D. G., Efficient and accurate approximations to the local coupled cluster singles doubles method using a truncated pair natural orbital basis. *Journal of Chemical Physics* **2009**, 131, 064103.
10. Hättig, C.; Klopper, W.; Köhn, A.; Tew, D. P., Explicitly Correlated Electrons in Molecules. *Chemical Reviews* **2012**, 112, 4-74.
11. Kong, L.; Bischoff, F. A.; Valeev, E. F., Explicitly Correlated R12/F12 Methods for Electronic Structure. *Chemical Reviews* **2012**, 112, 75-107.
12. Bross, D. H.; Hill, J. G.; Werner, H.-J.; Peterson, K. A., Explicitly correlated composite thermochemistry of transition metal species. *Journal of Chemical Physics* **2013**, 139, 094302.
13. Radoń, M., Spin-State Energetics of Heme-Related Models from DFT and Coupled Cluster Calculations. *Journal of Chemical Theory and Computation* **2014**, 10, 2306-2321.
14. Neese, F.; Liakos, D. G.; Ye, S., Correlated wavefunction methods in bioinorganic chemistry. *Journal of Biological Inorganic Chemistry* **2011**, 16, 821-829.
15. Jiang, W.; DeYonker, N. J.; Wilson, A. K., Multireference Character for 3d Transition-Metal-Containing Molecules. *Journal of Chemical Theory and Computation* **2012**, 8, 460-468.
16. White, S. R., Density matrix formulation for quantum renormalization groups. *Physical Review Letters* **1992**, 69, 2863-2866.
17. Keller, S. F.; Reiher, M., Determining Factors for the Accuracy of DMRG in Chemistry. *CHIMIA International Journal for Chemistry* **2014**, 68, 200-203.
18. Olivares-Amaya, R.; Hu, W.; Nakatani, N.; Sharma, S.; Yang, J.; Chan, G. K.-L., The ab-initio density matrix renormalization group in practice. *Journal of Chemical Physics* **2015**, 142, 034102.
19. Schollwöck, U., The density-matrix renormalization group in the age of matrix product states. *Annals of Physics* **2011**, 326, 96-192.
20. Chan, G. K.-L., An algorithm for large scale density matrix renormalization group calculations. *Journal of Chemical Physics* **2004**, 120, 3172-3178.
21. Moritz, G.; Reiher, M., Decomposition of density matrix renormalization group states into a Slater determinant basis. *Journal of Chemical Physics* **2007**, 126, 244109.
22. Keller, S.; Dolfi, M.; Troyer, M.; Reiher, M., An Efficient Matrix Product Operator Representation of the Quantum-Chemical Hamiltonian. *Journal of Chemical Physics* **2015**, 143, 244118.

23. Kurashige, Y.; Yanai, T., Second-order perturbation theory with a density matrix renormalization group self-consistent field reference function: Theory and application to the study of chromium dimer. *Journal of Chemical Physics* **2011**, 135, 094104.
24. Hedegård, E. D.; Knecht, S.; Kielberg, J. S.; Jensen, H. J. A.; Reiher, M., Density matrix renormalization group with efficient dynamical electron correlation through range separation. *Journal of Chemical Physics* **2015**, 142, 224108.
25. Neuscamman, E.; Yanai, T.; Chan, G. K.-L., A review of canonical transformation theory. *International Reviews in Physical Chemistry* **2010**, 29, 231-271.
26. Marti, K. H.; Reiher, M., The Density Matrix Renormalization Group Algorithm in Quantum Chemistry. *Zeitschrift für Physikalische Chemie* **2010**, 224, 583-599.
27. Chan, G. K.-L.; Sharma, S., The Density Matrix Renormalization Group in Quantum Chemistry. *Annual Review of Physical Chemistry* **2011**, 62, 465-481.
28. Wouters, S.; Van Neck, D., The density matrix renormalization group for ab initio quantum chemistry. *European Physical Journal D* **2014**, 68, 1-20.
29. Yanai, T.; Kurashige, Y.; Mizukami, W.; Chalupský, J.; Lan, T. N.; Saitow, M., Density matrix renormalization group for ab initio Calculations and associated dynamic correlation methods: A review of theory and applications. *International Journal of Quantum Chemistry* **2015**, 115, 283-299.
30. Szalay, S.; Pfeffer, M.; Murg, V.; Barcza, G.; Verstraete, F.; Schneider, R.; Legeza, Ö., Tensor product methods and entanglement optimization for ab initio quantum chemistry. *International Journal of Quantum Chemistry* **2015**, 115, 1342-1391.
31. Atanasov, M.; Daul, C. A., A DFT based ligand field model for magnetic exchange coupling in transition metal dimmer complexes: (i) principles. *Chemical Physics Letters* **2003**, 379, 209-215.
32. Atanasov, M.; Daul, C. A.; Rauzy, C. A DFT Based Ligand Field Theory. In *Optical Spectra and Chemical Bonding in Inorganic Compounds: Special Volume dedicated to Professor Jørgensen I*, Mingos, D. M. P.; Schönherr, T., Eds.; Springer Berlin Heidelberg: Berlin, Heidelberg, 2004, pp 97-125.
33. Daul, C., Density functional theory applied to the excited states of coordination compounds. *International Journal of Quantum Chemistry* **1994**, 52, 867-877.
34. Daul, C.; Zlatar, M.; Gruden-Pavlović, M.; Swart, M. Application of Density Functional and Density Functional Based Ligand Field Theory to Spin States. In *Spin States in Biochemistry and Inorganic Chemistry*; John Wiley & Sons, Ltd: 2015, pp 7-34.
35. Vlahović, F.; Perić, M.; Gruden-Pavlović, M.; Zlatar, M., Assessment of TD-DFT and LF-DFT for study of d − d transitions in first row transition metal hexaaqua complexes. *Journal of Chemical Physics* **2015**, 142, 214111.
36. Car, R.; Parrinello, M., Unified Approach for Molecular Dynamics and Density-Functional Theory. *Physical Review Letters* **1985**, 55, 2471-2474.
37. Richter, M.; Marquetand, P.; González-Vázquez, J.; Sola, I.; González, L., SHARC: ab Initio Molecular Dynamics with Surface Hopping in the Adiabatic Representation Including Arbitrary Couplings. *Journal of Chemical Theory and Computation* **2011**, 7, 1253-1258.
38. Marquetand, P.; Richter, M.; González-Vázquez, J.; Sola, I.; González, L., Nonadiabatic ab initio molecular dynamics including spin–orbit coupling and laser fields. *Faraday Discussions* **2011**, 153, 261-273.
39. Laio, A.; VandeVondele, J.; Rothlisberger, U., A Hamiltonian electrostatic coupling scheme for hybrid Car–Parrinello molecular dynamics simulations. *Journal of Chemical Physics* **2002**, 116, 6941-6947.
40. Brunk, E.; Rothlisberger, U., Mixed Quantum Mechanical/Molecular Mechanical Molecular Dynamics Simulations of Biological Systems in Ground and Electronically Excited States. *Chemical Reviews* **2015**, 115, 6217-6263.
41. Cascella, M.; Cuendet, M. A.; Tavernelli, I.; Rothlisberger, U., Optical Spectra of Cu(II)−Azurin by Hybrid TDDFT-Molecular Dynamics Simulations. *Journal of Physical Chemistry B* **2007**, 111, 10248-10252.
42. Comba, P.; Hambley, T. W.; Martin, B. Part Introduction. In *Molecular Modeling of Inorganic Compounds*; Wiley-VCH Verlag GmbH & Co. KGaA: 2009, pp 1-1.
43. Deeth, R. J.; Anastasi, A. E.; Wilcockson, M. J., An In Silico Design Tool for Fe(II) Spin Crossover and Light-Induced Excited Spin State-Trapped Complexes. *Journal of the American Chemical Society* **2010**, 132, 6876-6877.
44. Handley, C. M.; Deeth, R. J., A Multi-Objective Approach to Force Field Optimization: Structures and Spin State Energetics of d6 Fe(II) Complexes. *Journal of Chemical Theory and Computation* **2012**, 8, 194-202.

45. Foscato, M.; Deeth, R. J.; Jensen, V. R., Integration of Ligand Field Molecular Mechanics in Tinker. *Journal of Chemical Information and Modeling* **2015**, 55, 1282-1290.
46. Andersson, K.; Malmqvist, P. Å.; Roos, B. O., Second-order perturbation theory with a complete active space self-consistent field reference function. *Journal of Chemical Physics* **1992**, 96, 1218-1226.
47. Malmqvist, P. Å.; Pierloot, K.; Shahi, A. R. M.; Cramer, C. J.; Gagliardi, L., The restricted active space followed by second-order perturbation theory method: Theory and application to the study of CuO2 and Cu2O2 systems. *Journal of Chemical Physics* **2008**, 128, 204109.
48. Angeli, C.; Cimiraglia, R.; Evangelisti, S.; Leininger, T.; Malrieu, J.-P., Introduction of n-electron valence states for multireference perturbation theory. *Journal of Chemical Physics* **2001**, 114, 10252-10264.
49. Nakano, H.; Nakatani, J.; Hirao, K., Second-order quasi-degenerate perturbation theory with quasi-complete active space self-consistent field reference functions. *Journal of Chemical Physics* **2001**, 114, 1133-1141.
50. Forsberg, N.; Malmqvist, P.-Å., Multiconfiguration perturbation theory with imaginary level shift. *Chemical Physics Letters* **1997**, 274, 196-204.
51. Ghigo, G.; Roos, B. O.; Malmqvist, P.-Å., A modified definition of the zeroth-order Hamiltonian in multiconfigurational perturbation theory (CASPT2). *Chemical Physics Letters* **2004**, 396, 142-149.
52. Roos, B. O.; Taylor, P. R.; Si�doteq gbahn, P. E. M., A complete active space SCF method (CASSCF) using a density matrix formulated super-CI approach. *Chemical Physics* **1980**, 48, 157-173.
53. Malmqvist, P. A.; Rendell, A.; Roos, B. O., The restricted active space self-consistent-field method, implemented with a split graph unitary group approach. *Journal of Physical Chemistry* **1990**, 94, 5477-5482.
54. Vancoillie, S.; Zhao, H.; Tran, V. T.; Hendrickx, M. F. A.; Pierloot, K., Multiconfigurational Second-Order Perturbation Theory Restricted Active Space (RASPT2) Studies on Mononuclear First-Row Transition-Metal Systems. *Journal of Chemical Theory and Computation* **2011**, 7, 3961-3977.
55. Pierloot, K.; Zhao, H.; Vancoillie, S., Copper Corroles: the Question of Noninnocence. *Inorganic Chemistry* **2010**, 49, 10316-10329.
56. Chen, H.; Song, J.; Lai, W.; Wu, W.; Shaik, S., Multiple Low-Lying States for Compound I of P450cam and Chloroperoxidase Revealed from Multireference Ab Initio QM/MM Calculations. *Journal of Chemical Theory and Computation* **2010**, 6, 940-953.
57. Radoń, M.; Broclawik, E.; Pierloot, K., DFT and Ab Initio Study of Iron-Oxo Porphyrins: May They Have a Low-Lying Iron(V)-Oxo Electromer? *Journal of Chemical Theory and Computation* **2011**, 7, 898-908.
58. Zhao, H.; Pierloot, K.; Langner, E. H. G.; Swarts, J. C.; Conradie, J.; Ghosh, A., Low-Energy States of Manganese–Oxo Corrole and Corrolazine: Multiconfiguration Reference ab Initio Calculations. *Inorganic Chemistry* **2012**, 51, 4002-4006.
59. Aquilante, F.; Malmqvist, P.-Å.; Pedersen, T. B.; Ghosh, A.; Roos, B. O., Cholesky Decomposition-Based Multiconfiguration Second-Order Perturbation Theory (CD-CASPT2): Application to the Spin-State Energetics of CoIII(diiminato)(NPh). *Journal of Chemical Theory and Computation* **2008**, 4, 694-702.
60. Vancoillie, S.; Delcey, M. G.; Lindh, R.; Vysotskiy, V.; Malmqvist, P.-Å.; Veryazov, V., Parallelization of a multiconfigurational perturbation theory. *Journal of Computational Chemistry* **2013**, 34, 1937-1948.
61. Pierloot, K.; Vancoillie, S., Relative energy of the high-(T2g5) and low-(A1g1) spin states of [Fe(H2O)6]2+, [Fe(NH3)6]2+, and [Fe(bpy)3]2+: CASPT2 versus density functional theory. *Journal of Chemical Physics* **2006**, 125, 124303.
62. Vancoillie, S.; Zhao, H.; Radoń, M.; Pierloot, K., Performance of CASPT2 and DFT for Relative Spin-State Energetics of Heme Models. *Journal of Chemical Theory and Computation* **2010**, 6, 576-582.
63. Radoń, M.; Broclawik, E.; Pierloot, K., Electronic Structure of Selected (FeNO)7 Complexes in Heme and Non-Heme Architectures: A Density Functional and Multireference ab Initio Study. *Journal of Physical Chemistry B* **2010**, 114, 1518-1528.
64. Harris, R. K.; Becker, E. D.; Cabral de Menezes, S. M.; Goodfellow, R.; Granger, P., NMR nomenclature: nuclear spin properties and conventions for chemical shifts. IUPAC Recommendations 2001. International Union of Pure and Applied Chemistry. Physical Chemistry Division. Commission on Molecular Structure and Spectroscopy. *Magnetic Resonance in Chemistry* **2002**, 40, 489-505.
65. Markley, J. L.; Bax, A.; Arata, Y.; Hilbers, C. W.; Kaptein, R.; Sykes, B. D.; Wright, P. E.; Wüthrich, K., Recommendations for the presentation of NMR structures of proteins and nucleic acids – IUPAC-IUBMB-IUPAB Inter-Union Task Group on the Standardization of Data Bases of Protein and Nucleic Acid Structures Determined by NMR Spectroscopy. *Journal of Biomolecular NMR* **1998**, 12, 1-23.

66. Harris, R. K.; Becker, E. D.; de Menezes, S. M. C.; Granger, P.; Hoffman, R. E.; Zilm, K. W., Further conventions for NMR shielding and chemical shifts (IUPAC Recommendations 2008). *Pure and Applied Chemistry* **2008**, 80, 59–84.
67. Gutmanas, A.; Adams, P. D.; Bardiaux, B.; Berman, H. M.; Case, D. A.; Fogh, R. H.; Guntert, P.; Hendrickx, P. M. S.; Herrmann, T.; Kleywegt, G. J.; Kobayashi, N.; Lange, O. F.; Markley, J. L.; Montelione, G. T.; Nilges, M.; Ragan, T. J.; Schwieters, C. D.; Tejero, R.; Ulrich, E. L.; Velankar, S.; Vranken, W. F.; Wedell, J. R.; Westbrook, J.; Wishart, D. S.; Vuister, G. W., NMR Exchange Format: a unified and open standard for representation of NMR restraint data. *Nat Struct Mol Biol* **2015**, 22, 433-434.
68. Balland, V.; Banse, F.; Anxolabéhère-Mallart, E.; Ghiladi, M.; Mattioli, T. A.; Philouze, C.; Blondin, G.; Girerd, J.-J., Fe(II) and Fe(III) Mononuclear Complexes with a Pentadentate Ligand Built on the 1,3-Diaminopropane Unit. Structures and Spectroscopic and Electrochemical Properties. Reaction with H2O2. *Inorganic Chemistry* **2003**, 42, 2470-2477.
69. Paquete, C. M.; Saraiva, I. H.; Calcada, E.; Louro, R. O., Molecular Basis for Directional Electron Transfer. *Journal Of Biological Chemistry* **2010**, 285, 10370–10375.
70. Lazarides, T.; Sazanovich, I. V.; Simaan, A. J.; Kafentzi, M. C.; Delor, M.; Mekmouche, Y.; Faure, B.; Réglier, M.; Weinstein, J. A.; Coutsolelos, A. G.; Tron, T., Visible Light-Driven O2 Reduction by a Porphyrin–Laccase System. *Journal of the American Chemical Society* **2013**, 135, 3095-3103.
71. Dubois, L.; Caspar, R.; Jacquamet, L.; Petit, P.-E.; Charlot, M.-F.; Baffert, C.; Collomb, M.-N.; Deronzier, A.; Latour, J.-M., Binuclear Manganese Compounds of Potential Biological Significance. Part 2. Mechanistic Study of Hydrogen Peroxide Disproportionation by Dimanganese Complexes: The Two Oxygen Atoms of the Peroxide End up in a Dioxo Intermediate. *Inorganic Chemistry* **2003**, 42, 4817-4827.